Consciousness and Cognition 78 (2020) 102863

Contents lists available at ScienceDirect

Consciousness and Cognition

journal homepage: www.elsevier.com/locate/concog

Neuronal correlates of full and partial visual conscious perception

Hamed Haque[a,b,*], Muriel Lobier[a], J. Matias Palva[a,c,d], Satu Palva[a,c,*]

[a] Neuroscience Center, Helsinki Institute of Life Science, University of Helsinki, Finland
[b] BioMag Laboratory, HUS Medical Imaging Center, Finland
[c] Centre for Cognitive Neuroimaging, Institute of Neuroscience and Psychology, University of Glasgow, United Kingdom
[d] Department of Neuroscience and Biomedical Engineering, Aalto University, Finland

ARTICLE INFO

Keywords:
MEG
Conscious perception
Visual
Oscillations
Evoked response

ABSTRACT

Stimuli may induce only partial consciousness—an intermediate between null and full consciousness—where the presence but not identity of an object can be reported. The differences in the neuronal basis of full and partial consciousness are poorly understood. We investigated if evoked and oscillatory activity could dissociate full from partial conscious perception. We recorded human cortical activity with magnetoencephalography (MEG) during a visual perception task in which stimulus could be either partially or fully perceived. Partial consciousness was associated with an early increase in evoked activity and theta/low-alpha-band oscillations while full consciousness was also associated with late evoked activity and beta-band oscillations. Full from partial consciousness was dissociated by stronger evoked activity and late increase in theta oscillations that were localized to higher-order visual regions and posterior parietal and prefrontal cortices. Our results reveal both evoked activity and theta oscillations dissociate partial and full consciousness.

1. Introduction

Conscious perception has been suggested to be an all-or-none process, where one can only be either fully aware or completely unaware of a stimulus' contents (Grill-Spector & Kanwisher, 2005; Sekar, Findley, Poeppel, & Llinas, 2013; Sergent & Dehaene, 2004a) or a graded phenomenon, where one's perception of a stimulus can be incomplete and imperfect (Elliott, Baird, & Giesbrecht, 2016; Kouider, De Gardelle, Sackur, & Dupoux, 2010; Nieuwenhuis & de Kleijn, 2011; Overgaard, Rote, Mouridsen, & Ramsøy, 2006; Sandberg, Timmermans, Overgaard, & Cleeremans, 2010). A large part of the literature on visual perception has concentrated on unraveling the neural correlates of consciousness (NCC) by elucidating the differences in neural activity for seen and unseen stimuli presented at perceptual threshold using electrophysiological recordings that reveal neuronal activity with millisecond precision. These studies using non-invasive electroencephalography (EEG) (Sergent, Baillet, & Dehaene, 2005; Fahrenfort, Scholte, & Lamme, 2007; Koivisto et al., 2008; Eklund & Wiens, 2018), magnetoencephalography (MEG) (Jones, Pritchett, Stufflebeam, Hamalainen, & Moore, 2007; Melloni, Schwiedrzik, Muller, Rodriguez, & Singer, 2011; Palva, Linkenkaer-Hansen, Naatanen, & Palva, 2005) as well as intracranial EEG (iEEG) (Fisch et al., 2009; Gaillard et al., 2009) recordings have shown that the strength of event-related activity is positively correlated with conscious sensory perception. The amplitudes of local gamma (30–120 Hz) oscillations, both in MEG sensor-level analyses (Palva, Linkenkaer-Hansen et al., 2005; Wyart & Tallon-Baudry, 2008) and iEEG (Aru et al., 2012; Fisch et al., 2009; Gaillard et al., 2009; Vidal et al., 2014; Vidal, Perrone-Bertolotti, Kahane, & Lachaux, 2015), have also been shown to correlate with conscious perception of visual stimuli.

* Corresponding authors at: Helsinki Institute of Life Science, Neuroscience Center, University of Helsinki, Finland.
E-mail addresses: hamed.haque@helsinki.fi (H. Haque), satu.palva@helsinki.fi, satu.palva@glasgow.ac.uk (S. Palva).

https://doi.org/10.1016/j.concog.2019.102863
Received 5 July 2019; Received in revised form 17 December 2019; Accepted 18 December 2019

Only few studies have, however, investigated how neuronal activity is modulated by the degree of awareness achieved and the neural mechanisms responsible for putative graded perception are debated (Christensen, Ramsøy, Lund, Madsen, & Rowe, 2006; Tagliabue, Mazzi, Bagattini, & Savazzi, 2016). One model proposes that consciousness is composed of two distinct processes: phenomenal consciousness—the perception of the actual content, and access consciousness—the ability to report, use or act upon the percept (Block, 2005). The alternative partial awareness hypothesis (Kouider et al., 2010) posits that visual information is processed through a hierarchy of representations and that levels of awareness depend on which representational levels can be accessed. In line with this hypothesis, when participants rate the subjective visibility of simple geometric figures presented for different durations using the four level Perceptual Awareness Scale (PAS) (Ramsøy & Overgaard, 2004), the resulting psychometric functions display a shallow slope, consistent with a gradual transition between no awareness and full awareness (Overgaard et al., 2006; Sandberg et al., 2010; Sandberg, Bibby, Timmermans, Cleeremans, & Overgaard, 2011). In fMRI data, gradual increases in visibility are linked to gradual increases in activity in fronto-parietal areas such as the intra-parietal sulcus (IPS), the precentral gyrus and the insula (Christensen et al., 2006). FMRI evidence also suggest that visibility of low-level visual stimuli is reflected in cortical activity in both lower and higher order visual cortex (Imamoglu, Heinzle, Imfeld, & Haynes, 2014). In EEG data, the visual awareness negativity (VAN) has been associated with detection of visual stimuli (detection without identification) but not with discrimination of visual stimuli (discrimination with correct identification) (Koivisto, Grassini, Salminen-Vaparanta, & Revonsuo, 2017). Furthermore, although the strength of local gamma oscillations is correlated with awareness, in iEEG recordings the mere presence of gamma oscillations signals the content of visual information but is not sufficient for conscious perception (Aru et al., 2012; Vidal et al., 2014). This supports the idea of different neuronal underpinnings for full and partial consciousness.

We hypothesized that the neuronal underpinnings for full and partial consciousness would be reflected in the strength of evoked responses and especially in the strength of induced oscillatory activity. To investigate the neuronal correlates of partial and full consciousness, we recorded human cortical activity with MEG during a threshold detection task in which participants detected either only the presence but not the identity of visual stimuli or both the presence and identity of visual stimuli. Different perceptual outcomes for physically similar stimuli can be achieved by using masks (Del Cul, Baillet, & Dehaene, 2007), varying stimulus intensity (Wyart & Tallon-Baudry, 2008) or using visual stimuli at individually determined perceptual threshold levels. In this study, we used a combination of the latter two methods by asking participants to discriminate between two geometric shapes embedded in dynamic noise at two independent and individually titrated thresholds for partial and full consciousness. Participants first made their perceptual decision and then rated stimulus visibility using a four level PAS scale (Ramsøy & Overgaard, 2004). We then compared the evoked and oscillatory activity in source-localized MEG data between visual stimuli that were fully perceived, partially perceived or not perceived to identify the distinct neuronal correlates of partial and full consciousness.

2. Material and methods

We used a data-driven analyses approach that reveals only the most robust effects in the data, regardless of whether they were or were not the original hypothesis and as such provides a more rigorous testing for the hypothesis. The analyses were performed on a well-validated and established data-driven analysis workflow used in several prior publications by the research group (Hirvonen & Palva, 2016; Honkanen, Rouhinen, Wang, Palva, & Palva, 2015; Kulashekhar, Pekkola, Palva, & Palva, 2016; Palva, 2005; Palva, Kulashekhar, Hamalainen, & Palva, 2011; Rouhinen, Panula, Palva, & Palva, 2013). All data analyses, where not indicated otherwise, were performed on a LabVIEW-based (National Instruments) in-house developed neuroinformatics platform. The usage of the platform is available upon request. The python code used to perform the cluster-based permutation analysis of the evoked MEG data can be found on GitHub (https://github.com/palvalab/visual-perception). The task and MEG recordings of the data analyzed here are described in detail in Lobier, Palva, and Palva (2017).

2.1. Participants and data acquisition

Magnetoencephalography (MEG) data were recorded from fourteen healthy participants (mean: 26.4 years old, range: 20–33; seven females) with normal or corrected to normal vision using a 306 channel MEG instrument composed of 204 planar gradiometers and 102 magnetometers (Elekta Neuromag, Helsinki, Finland) at 600 Hz sampling rate. Source reconstruction was unsuccessful for one participant who was therefore excluded from all data analysis. T1-weighted anatomical MRI scans for cortical surface reconstruction models were obtained for each subject at a resolution of $1 \times 1 \times 1$ mm (MP-RAGE) with a 1.5-T MRI scanner (Siemens, Germany). The study was performed according to the Declaration of Helsinki and approved by an ethical committee of the Helsinki University Central Hospital. Participants gave written informed consent on participation before the experiment.

2.2. Task and stimuli

We used MATLAB and Psychtoolbox-3 (Brainard, 1997) to generate the stimuli and task. Participants carried out a stimulus discrimination task between two possible visual shapes (Fig. 1A). First, participants fixated on a red fixation cross (1° of visual angle) centered in a circular patch of dynamic grayscale Perlin noise (diameter = 10°). After a jittered duration of 1.25 ± 0.25 s, the color of the left or right half of the fixation cross changed from red to green, cuing participants to attend to either the left or right hemifield. One of two geometrical shapes (at 2°) was displayed for 0.1 s in the attended or non-attended lower quadrant 1.25 ± 0.25 s after cue onset. Trials could be valid (73%, stimulus displayed in the attended hemifield), invalid (18%, stimulus displayed in the non-attended hemifield) or catch (9%, no stimulus displayed). Participants were asked to respond to both valid and invalid trials. Catch trials were

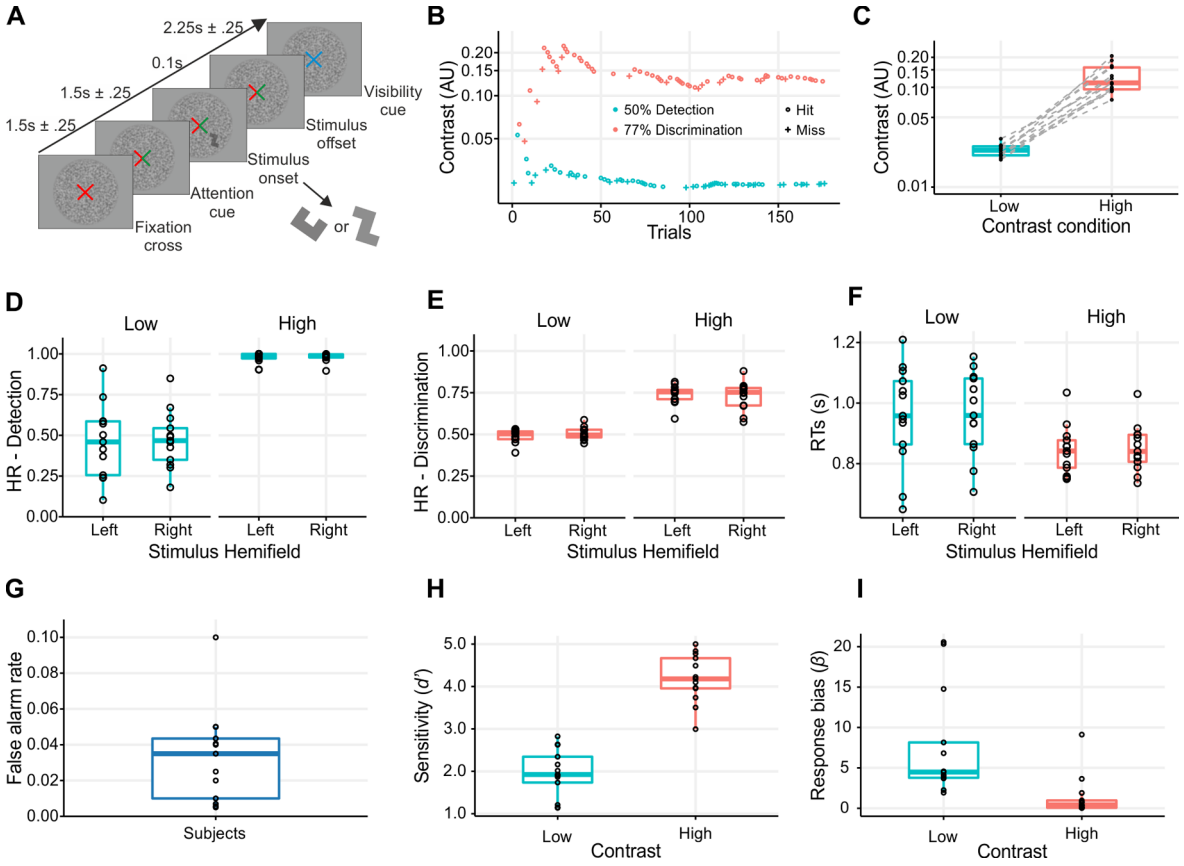

Fig. 1. Behavioral results indicate that low contrast detection reflects partial consciousness while high contrast discrimination reflects full consciousness. **(A)** Schematics of the experimental paradigm. Participants were cued to attend to the right or left hemifield by a change from red to green of the relevant half of a central fixation cross. The attention cue remained on screen for the entire duration of the trial. After 1.25 ± 0.25 s, one of two geometrical shapes was displayed for 0.1 s in the attended or non-attended lower hemifield at either low or high contrast. Participants were asked to discriminate between these two geometrical shapes regardless of the stimulus location. After the central fixation cross changed to blue, participants were asked to rate stimulus visibility on a four-level scale (not visible, barely visible, partially visible, fully visible). **(B)** Performance of a representative participant during the thresholding procedure. Each data point represents the contrast strength of a trial, drawn in trial chronological order from left to right. For data points from the 50% detection staircase, Hits represent seen stimuli and Misses unseen stimuli. For data points from the 77% discrimination staircase, Hits represent correctly identified trials and Misses represent incorrectly identified trials. **(C)** Distribution of contrast strengths for the Low and High contrast conditions. Dashed lines indicate change in contrast strength for each participant between the two contrast conditions. **(D)** Individual Detection Hit-Rates (HR) for low and high contrast stimuli. **(E)** Individual Discrimination Hit-Rates (HR) for low and high contrast stimuli. **(F)** Individual average Reaction Times (RT) for low and high contrast stimuli. **(G)** Individual false-alarm rates for all subjects. **(H)** Individual sensitivity (d′) for low and high contrast stimuli. Sensitivity (d′) measures the distance between the means of the signal and noise distributions. **I.** Individual response bias (β) for low and high contrast stimuli. Larger β values indicate a tendency to report stimuli as undetected. (For interpretation of the references to color in this figure legend, the reader is referred to the web version of this article.)

used to calculate the false-alarm rate and ensure that participants were complying with task instructions (*i.e.*, correctly withholding response when no stimulus was present). Stimulus hemifield, contrast strength and trial type were pseudorandomized across trials and participants. Participants were asked to indicate as accurately and quickly as possible which shape they had perceived by a thumb lift and asked not to respond if they had not perceived any stimulus. Thumb and finger lifts were recorded via hand-held fiber optic response pads. The shape assigned to each thumb was counterbalanced across participants. 2.15 ± 0.25 s after stimulus onset, the color of the fixation cross changed to blue and participants were asked to rate stimulus visibility on a four level scale (not visible, barely visible, partially visible, and fully visible) using finger lifts. During the experiment, participants were instructed to maintain fixation on the fixation cross during the entire trial and eye movements were monitored using electrooculography (EOG).

To investigate partial and full consciousness, stimuli were displayed at two different contrast strengths. Contrast strengths were calibrated individually at the beginning of the first recording session using the Palamedes toolbox implementation of the QUEST algorithm. Participants took part in a one hour training session 24 to 48 h before the first recording session to ensure that they were familiar and comfortable with the task and that perceptual learning effects did not affect contrast strength calibration. Low contrast stimuli were calibrated to a 50% detection rate (participant perceived/detected a shape, irrespective of which one—partial consciousness) and High contrast stimuli were calibrated to a 77% correct discrimination rate (participant perceived/discriminated the

correct shape—full consciousness). In both cases only attended trials were used for calibration purposes. For the MEG experiment, high and low-contrast stimuli were presented in random order in sets of 88 trials, each set lasting 12 min. Each participant participated in four recording sessions, each held on a different day, resulting in a total of 20–25 sets of 88 trials. The average number of trials collected per participant, including all conditions and before artifact rejection, was 2120 (range 1584–2220).

2.3. Analysis of behavioral data

We computed reactions times (RTs), detection hit-rates (DET-HR) and discrimination hit-rates (DISC-HR) for each contrast strength for Low contrast (partial consciousness) and High contrast (full consciousness) and stimulus hemifield (Left and Right) using attended trials only. DET-HR was computed as the proportion of detected stimuli, regardless of discrimination accuracy. DISC-HR was computed as the proportion of detected stimuli that were correctly discriminated. For stimulus detection, we computed measures of signal detection theory: false alarm rate, d prime and beta (Stanislaw & Todorov, 1999). We reported Bayes factors –BF01- (Rouder, Speckman, Sun, Morey, & Iverson, 2009) expressing the probability of the data given H0 (absence of an effect) relative to H1 (presence of an effect). BF01 values larger than 1 are therefore in favor of H0. Bayes factors were computed using the R package BayesFactor. For the Bayes factor analysis, an uninformative Jeffreys prior was placed on the variance of the normal population, while a Cauchy prior with scale parameter of $r = \sqrt{2}/2$ was placed on the standardized effect size. By using Bayes factor analysis, we tested whether DISC-HR and DET-HR were different from chance level for low contrast stimuli. We then compared performance between right and left hemifields for other conditions. To test whether discrimination performance was different between high and low contrasts, we used a repeated-measure 2×2 ANOVA with hemifield and contrast as within-subject factors. Hit-rates were transformed with the arcsine square root before statistical analysis to stabilize variances, normalize proportional data and meet the assumptions of ANOVA (Sokal & Rohlf, 1995).

2.4. MEG data preprocessing, and collapsing data into trials

We applied the temporal extension of signal space separation methods (tSSS) (Taulu, Simola, & Kajola, 2005) with MaxFilter (Elekta Neuromag) to the raw signal to suppress extra-cranial noise, interpolate bad channels and co-localize recordings in signal space individually for each participant. Using independent component analysis (ICA, MATLAB toolbox Fieldtrip, http://fieldtrip.fcdonders.nl, (Oostenveld, Fries, Maris, & Schoffelen, 2011)), we extracted and identified components that were correlated with ocular artefacts (identified using the EOG signal) or heart-beat artefacts (identified using the magnetometer signal as a reference). The pre-processed MEG sensor time-series were epoched into individual trials of 1800 ms, spanning from −800 ms pre-stimulus onset to 1000 ms post-stimulus. We rejected all trials that were contaminated by eye movements or muscle activity. These epoched trials were subsequently used when computing the evoked response (Section 2.6) and oscillation amplitudes (Section 2.7).

2.5. MEG source reconstruction and creation of surface parcellations

We used Freesurfer software (Fischl, 2012) to carry out volumetric segmentation of the MRI data, surface reconstruction, flattening, and cortical parcellation/labeling with the Freesurfer/Destrieux atlas (Destrieux, Fischl, Dale, & Halgren, 2010). We then used MNE software (http://www.nmr.mgh.harvard.edu/martinos/userInfo/data/sofMNE.php) (Gramfort et al., 2014) to create single-layer boundary element conductivity models and cortically constrained source models for the MEG-MRI co-localization and for the preparation of the forward and inverse operators (Dale et al., 2000). Source model dipoles were of fixed orientation (normal to the pial surface) and located on a 5 mm resolution grid. Individual source models thus contained 11,000–14,000 source vertices.

The preprocessed MEG time-series was epoched from 500 ms to 1000 ms from visibility cue onset of all trials and broadband filtered using a finite impulse response (FIR) from 1 to 45 Hz, to compute noise covariance matrices (NCMs). We used minimum-norm estimate (MNE) in the form of dynamic statistical parametric map (dSPM) operators (Dale et al., 2000) that were built from the NCMs and used 0.05 as the regularization constant. Individual broadband inverse operators were then computed from these NCMs using MNE software and used to project the sensor-space data into source-space. These source-space vertices were then collapsed into 400 cortical parcels. The parcels were constructed by iteratively splitting the largest parcel of individual Destrieux parcellations (148 parcels) (Destrieux et al., 2010) along a previously determined axis. Axes were determined pre-emptively using the fsaverage brain in Freesurfer. For each to-be-split parcel, the splitting axis was defined as the first principal component of the parcel. Splitting was carried out until 400 parcels were defined. By using parcels and neuro-anatomical labels, we eliminate the need for inter-subject morphing for group-level analyses (Hirvonen & Palva, 2016; Honkanen et al., 2015; Palva et al., 2011). Collapsing was carried out using sparse fidelity-optimized collapse operators that maximized the reconstruction accuracy in each subject's individual source space (Korhonen, Palva, & Palva, 2014). The analyses were carried out in the 400 cortical parcels to allow maximal individual functional cortical separability and robust optimization of the source-collapsing approach.

2.6. Evoked broadband activity analysis

For estimating the evoked response (ER), for each parcel, we used the epoched MEG time-series which was 1–45 Hz broad-band filtered and decimated to 300 Hz (as in (Hirvonen & Palva, 2016)). We then computed from the parcel-collapsed broad-band filtered time-series, the individual trial-averaged evoked response by applying a moving average of 5 samples. We computed ERs separately for each condition but using only trials in which the stimulus was presented in the attended hemifield to avoid confounding effects of

visuospatial attention. We first excluded trials with eye blinks in the peri-stimulus interval or eye movements in the post-stimulus interval and next equalized the number of trials within condition pairs individually for each participant by removing trials from the condition with greater number of trials, until both conditions had the same number of trials. This was done by comparing the onset latencies of trials in both conditions, and removing trials with the largest difference between the latencies.

Before statistical testing, time-series were baseline corrected by subtracting the average pre-stimulus activity (-500 to -100 ms) and collapsed into a coarser parcellation of 200 parcels to limit the number of comparisons and to improve statistical stability by averaging out anatomical variability that is large across individuals (Hirvonen & Palva, 2016; Honkanen et al., 2015; Palva et al., 2011). Group-level statistics were performed on the resulting time-series separately for each contrast and parcel using a cluster-based random permutation approach (Maris & Oostenveld, 2007) performed in MNE-python (https://mne.tools/stable/index.html) such that within a given parcel, a paired *t*-test was performed at each time-point, but not across anatomy. All contiguous time-points exceeding a significance level of $\alpha = 0.01$ were grouped into clusters. The cluster-level statistic of each cluster were then defined as the sum of the t-values within the cluster. This approach controls the type-1 error rate in the presence of multiple comparisons across time-points. We then created a null distribution of the cluster-level statistics using permutations. We randomly assigned the conditions in subjects 1000 times, each time computing the largest cluster-level statistic for the permutation. We then used this null distribution to classify clusters falling in the highest or lowest 0.5th percentile as significant. The cluster-based permutation analyses were used to group effects by time and clusters deemed significant in the time-series of a parcel were independent of the time-series of adjacent parcels. Lastly, to summarize our data and results in an unbiased manner, we adopted and modified a measure of connection density (*K*) from network neuroscience (Bullmore & Sporns, 2009) and computed the fraction of cortical parcels that showed a significant amplitude increase (*cf.* with *K* used to represent fraction of connections).

2.7. Estimation of induced oscillatory amplitudes

To investigate whether full and/or partial conscious perception were associated with a modulation of local oscillation amplitudes, we filtered the epochs into 31 logarithmically spaced frequencies between 3 and 120 Hz using Morlet wavelets with a time–frequency compromise parameter of $m = 5$. The Morlet filtered signals were then decimated to a frequency-dependent sampling rate (5 samples per cycle/sampling frequency = 5 × filtering frequency). We computed induced oscillation amplitudes for each Morlet-wavelet frequency by averaging amplitudes across all trials (N) and (T) and overlapping 100 ms time-windows with a 50 ms overlap such that

$$A_P = \frac{1}{N \times T} \sum_{n,t} A(P, n, t)$$

where A_p is the amplitude within a parcel, N is the number of trials and T is the number of time-windows (Hirvonen & Palva, 2016; Honkanen et al., 2015; Palva et al., 2011). Averaged amplitudes were computed separately for each parcel and conditions.

2.8. Statistical analysis and visualization

Before statistical testing, amplitude data were baseline corrected by computing the logarithm of the baseline corrected amplitude: $A_P^{corr} = \log_{10}\left(\frac{A_P}{A_{P,baseline}}\right)$. Data were then collapsed to a coarser parcellation of 200 parcels to reduce the family-wise error by limiting the number of comparisons and to improve statistical stability due variability in brain functional anatomy, that is large across individuals (Hirvonen & Palva, 2016; Honkanen et al., 2015; Palva et al., 2011). Group statistics were subsequently performed separately for each frequency and time-window. Significant differences in parcel oscillation amplitudes were estimated using a Wilcoxon Signed Rank test with $\alpha = 0.05$. To remove false positives (FP) caused by multiple statistical tests, we pooled all significant observations over all parcels and then discarded as many of the least-significant comparisons as would predicted to be false discoveries by the alpha-level used in the corresponding test under the null-hypothesis. In addition to this false discovery rate (FDR) correction, for any given parcel, we only considered as significant time-frequency bins that were statistically significant in three consecutive overlapping time-windows (*i.e.*, 200 ms) as true neuronal activity was not expected to be as transient. This approach hence removed further FPs from the data.

To summarize our results, we first computed the fraction of significant parcels (P+) as a function of time, similarly to that for the evoked responses. To further remove the remaining FP findings from these summary data, we resampled the data using the leave-one-out jackknife method (Rodgers, 1999) to estimate the variability of the data. The leave-one-out jackknife approach is suitable for confirming the stability of observations and ensure that they are not driven by FPs, as demonstrated previously in Siebenhühner et al. (2016). To this end, we computed the fraction of significant parcels (P+) at each time-point for each jackknifed sample. The change of P+ across time for the full and jackknifed data was visualized together with the fraction of significant parcels to give confidence limits to these data.

We visualized amplitude modulations across frequencies using amplitude time-frequency representations (TFRs) for each contrast. For each TF bin, we computed the fraction of cortical parcels that showed a significant amplitude increase (*i.e.*, P+, the fraction of significant positive parcels for each TF bin) or decrease (*i.e.*, P−, the fraction of significant negative parcels for each TF bin). We localized the amplitude response for time-frequency windows showing responses of interest.

2.9. Visualization of neuronal activity in brain anatomy

Finally, we visualized the time windows for evoked activity and time-frequency windows for oscillatory activity of interest. Data was averaged over the selected regions of interest and the parcels with the significant effects were visualized on an inflated cortical surface. The color of the significant parcels reflected the average strength of the ER or amplitudes over the selected time window. To support the interpretation of the results in terms of the functional subdivisions of the cortical surface, prior fMRI studies (Kravitz, Saleem, Baker, Ungerleider, & Mishkin, 2013; Moradi et al., 2003) were used to link between the structural and functional anatomy. Tentative boundaries of the primary visual cortex (V1) was mapped to occipital pole and calcarine sulcus, and extrastriate visual cortex (V2) to the lingual gyrus and cuneus. The frontal eye fields (FEF) were mapped to the superior precentral sulcus. To identify brain regions putatively supporting attentional or executive control functions, we used the boundaries of dorsal attention and fronto-parietal networks defined by fMRI intrinsic connectivity patterns (Yeo et al., 2011).

3. Results

3.1. Behavioral results

Stimulus contrast strength was calibrated using two separate but interleaved Bayesian staircases to achieve 50% detection for low contrast stimuli and 77% discrimination for high contrast stimuli. In all participants, Bayesian staircases converged towards distinct contrast threshold values (see Fig. 1B for the thresholding data from a representative participant). At the group level (Fig. 1C), high contrast strength (mean = 0.13, bias-corrected and accelerated [Bca] 95%CI = [0.11–0.15]) was significantly greater than low contrast strength (mean = 0.023, Bca 95%CI = [0.022–0.025]) ($t(12) = 9.29$, $p = 7.9{\cdot}10^{-7}$, paired one-sample *t*-test).

We computed for each contrast strength (High and Low) and stimulus hemifield (Left and Right) three behavioral measures: proportion of detected stimuli (DET-HR) (Fig. 1D), proportion of correctly discriminated stimuli (DISC-HR) (Fig. 1E) and reaction times (RTs) (Fig. 1F), for attended trials only. Low contrast stimuli were calibrated to a 50% detection rate and this was reflected in the mean ± SD of DET-HR, which was 0.51 ± 0.21 for stimuli in the left hemifield and 0.523 ± 0.173 for stimuli in the right hemifield. DISC-HR for low contrast was at chance level for all subjects (Left: 0.504 ± 0.031, Right: 0.508 ± 0.039) which indicates that participants were able to detect but not discriminate the low-contrast stimuli. Bayes Factor analysis showed that discrimination performance was at chance level for low contrast stimuli regardless of hemifield (Left, BF01 = 3.4; Right, BF01 = 4.5). These stimuli can thus be considered to be partially but not fully consciously perceived, consistent with prior studies of partial conscious perception (Christensen et al., 2006; Imamoglu et al., 2014). For high contrast stimuli, DET-HR was at ceiling (Left: 0.978 ± 0.035, Right: 0.975 ± 0.037) while the DISC-HR matched the 77% discrimination rate targeted during calibration (Left: 0.735 ± 0.062, Right: 0.728 ± 0.083). High contrast stimuli were therefore fully perceived.

The false alarm rate was very low (0.035 ± 0.024), which indicates that the participants were able to avoid providing a response during catch trials where no stimulus was displayed (Fig. 1G). Sensitivity, or *d′* (d-prime), measures the distance between the means of the signal and noise distributions. *d′* for detection of low contrast stimuli was 1.96 ± 0.54 and for high contrast stimuli was 4.19 ± 0.55 (Fig. 1H). The *d′* for high contrast was significantly larger than for low contrast ($t(13) = 12.47$, $p = 3.14{\cdot}10^{-8}$, repeated-measures *t*-test), and indicates that participants were able to better distinguish between stimuli and catch trials when stimuli were presented at the high contrast than in the low contrast.

Beta (β), a measure of response bias, reflects the minimum level of internal certainty needed to decide that a stimulus was present, with larger values indicating a tendency to report stimuli as undetected. β was greater for low contrast (7.65 ± 6.31) than for high contrast stimuli (1.41 ± 2.43) ($t(13) = 4.57$, $p = 6.41{\cdot}10^{-4}$, repeated-measures *t*-test) (Fig. 1I). The participants were more likely to report high contrast stimuli as detected, than low contrast stimuli.

We used Bayes Factor analysis to determine whether performance was consistent between hemifields. For low contrast stimuli, DET-HR and DISC-HR did not differ between left and right hemifield stimuli (DET-HR: BF01 = 3.9; DISC-HR: BF01 = 3.5). For high contrast stimuli, DET-HR and DISC-HR also did not differ between left and right hemifield stimuli (DET-HR: BF01 = 3.0; DISC-HR: BF01 = 4.3). Reaction-times were similar for right and left hemifield stimuli for both contrast strengths (Low contrast, BF01 = 4.3; High contrast, BF01 = 2.8). These data indicate that participant performance was similar in both hemifields. Since behavioral performance did not differ between hemifields, we combined MEG data of right and left hemifield stimuli trials for subsequent analyses of brain activity.

Lastly, we investigated whether performance was consistent with partial consciousness for low contrast stimuli and full consciousness for high contrast stimuli. Bayes Factor analysis showed that discrimination performance differed for low and high contrast stimuli, regardless of hemifield (Left, BF01 = $3.5{\cdot}10^{-6}$; Right, BF01 = $4.6{\cdot}10^{-6}$). We also tested whether discrimination performance was different between high and low contrasts using a repeated-measure 2 × 2 ANOVA with hemifield and contrast as within-subject factors. Hit-rates were transformed with the arcsine square root before statistical analysis. Discrimination performance was significantly different between low contrast stimuli (mean = 0.50, Bca 95%CI = [0.48–0.51]) and high contrast stimuli (mean = 0.74, Bca 95%CI = [0.69–0.77]) (significant main effect of contrast: $F(1,12) = 134$, $p = 7.3{\cdot}10^{-8}$ $\eta^2 = 0.8$). The main effect of stimulus hemifield and the contrast × hemifield interaction were not significant ($p > .1$).

3.2. Amplification of evoked activity differentiates between Null, Partial, and full conscious perception

We first estimated whether the evoked responses (ERs) were correlated with partial conscious perception and full conscious visual

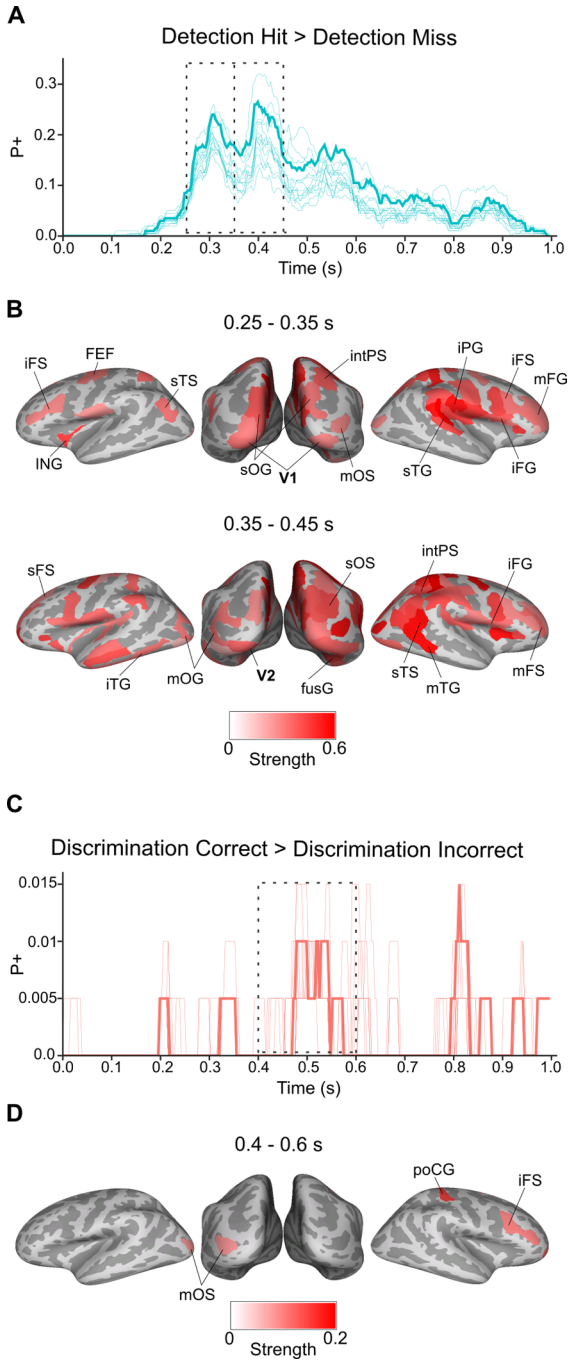

Fig. 2. *ERs are strengthened with partial consciousness and object discrimination.* **(A)** A fraction of the 200 brain areas (parcels) in which the evoked responses (ERs) during Detection Hit trials were stronger compared to Detection Miss trials (*T*-test, $p < .01$, cluster corrected). Thick lines represent results obtained with the full dataset while thin lines represent results obtained with leave-one-out jackknifing resampling. Time is displayed on the *x-axis* and the proportion of parcels with significant positive (P+) response on the *y-axis*. **(B)** The cortical areas in which evoked activity was stronger for Detection Hit trials compared to Detection Miss trials, displayed on an inflated three-dimensional cortical surface. Colors of the parcels indicate average strength of the evoked activity over the 0.25–0.35 s and 0.35–0.45 s time windows. **(C)** A fraction of the parcels in which ERs were stronger for Correct Discrimination compared to Incorrect Discrimination (T-test, $p < .05$, cluster corrected). **(D)** The cortical areas in which evoked activity was stronger for Discrimination Correct trials compared to Discrimination Incorrect trials. Colors of the parcels indicate average strength of the evoked activity over the 0.4–0.6 s time window. Parcels are indicated with acronyms: inferior frontal sulcus (iFS), frontal eye fields (FEF), insular gyrus (ING), superior temporal sulcus (sTS), superior occipital gyrus (sOG), primary visual cortex (V1), middle occipital sulcus (mOS), intraparietal sulcus (intPS), superior temporal gyrus (sTG), inferior parietal gyrus (iPG), inferior frontal gyrus (iFG), middle frontal gyrus (mFG), superior frontal sulcus (sFS), inferior temporal gyrus (iTG), middle occipital gyrus (mOG), secondary visual cortex (V2), fusiform gyrus (fusG), superior occipital sulcus (sOS), middle temporal gyrus (mTG), middle frontal sulcus (mFS), postcentral gyrus (poCG), superior frontal gyrus (sFG), and fronto-marginal gyrus (mrgF).

perception. As visual processing is lateralized to the contralateral visual cortex during early processing stages, we estimated the fraction of parcels that were significantly stronger (P+) for detected and undetected stimuli compared to baseline for the full dataset (thick line) and for each jack-knifed sample (thin lines) separately for stimuli presented to the left and right hemifield, as well as averaged over both stimuli (Fig. S1). ERs were clearly visible and very similar for all stimulus combinations. Also the fraction of parcels that showed stronger activity for the detected than undetected stimuli were similar for stimuli presented to the left and right hemifields and also did not show clear hemispheric lateralization (Fig. S2). The same pattern was observed for discriminated stimuli, incorrectly discriminated stimuli, and their comparison (Figs. S1 and S2). These data suggest that extensive hemispheric connectivity rapidly leads to bilateral processing of visual information. Due to the similarity of the behavioral and ER data, we combined trials for stimuli presented in the left and right hemifields in all subsequent analysis.

We next computed the correlation of ERs with partial consciousness. Detection Hit > Detection Miss contrast (Fig. 2A) showed a difference in the ERs from 0.2 s onwards, with the number of significant parcels increasing steadily, and peaking at 0.3 s and 0.4 s with over 20% and 25% of brain regions displaying significantly increased activity (226 ± 90 trials for each subject, mean ± SD). ERs were stronger for the detected than undetected stimuli in several parcels of the visual system as well as in several parcels of the posterior parietal cortex (PPC) and lateral prefrontal cortices (lPFC) (Fig. 2B). In the visual system, ERs were stronger in the parcels functionally part of V1/V2, as well as in the ventral visual stream regions such as superior occipital gyrus (sOG), and middle occipital sulcus (mOS) in the occipital cortex. In the PPC, intraparietal sulcus (intPS) and in the lPFC, inferior frontal gurys (iFG), middle frontal gyrus/sulcus (mFG/S) and superior precentral sulcus, corresponding functionally to frontal eye fields (FEF), also showed increased evoked activity for Hits compared to Misses.

To assess the neural correlates of full consciousness and, specifically, the ability to discriminate two distinct visual stimuli, we compared cortical responses between trials in which stimuli were correctly discriminated (Discrimination Correct) and those in which they were not (Discrimination Incorrect) for high contrast trials (179 ± 60 trials for each subject) (Fig. 2C). Only few cortical areas displayed significantly stronger activity in Discrimination Correct compared to Discrimination Incorrect trials, with the activity peaking at 0.5 s and 0.8 s (Fig. 2D). Stronger evoked responses for the correctly discriminated trials were found in the middle occipital sulcus (mOS) of the visual system, postcentral gyrus (poCG) of the PPC, and iFS of the lPFC.

3.3. Partial consciousness is associated with alpha and beta band amplitude modulations

We next investigated how oscillation amplitudes were modulated by partial and full conscious perception. All stimuli were followed by a sustained increase in the theta/low-alpha- (3–10 Hz) band amplitudes and a concurrent wide-band amplitude suppression between 10–50 Hz (Fig. 3A and B). These modulations were stronger for detected and undetected stimuli and hence correlated with partial consciousness (Fig. 3A). However, neither these modulations nor late onset amplitude increase in the beta band (15–20 Hz) differentiated correctly discriminated from undiscriminated stimuli (the stimuli could be of two different shapes) (Fig. 3B).

As the detected and undetected stimuli differed not only by conscious perception, but could also be confounded by a response requirement and motor action that was demanded (Tsuchiya, Wilke, Frässle, & Lamme, 2015), we next confirmed that the differences in neural responses were not related to motor processing. We divided the responses within each subject into 'fast' (0.785 ± 0.126 s, mean ± SD across subjects) and 'slow' (1.116 ± 0.168 s) response categories by the individual median RT (0.907 ± 0.144 s across subjects). We then estimated the strength of the evoked responses and oscillatory amplitudes separately for the two response categories, compared to when the stimuli was not detected (141 ± 54 trials for each subject) (Fig. 4). The Detection Miss trials used for both comparisons were the same. For fast and slow responses, the evoked responses and oscillation amplitude dynamics did not differ significantly. This indicates that both the increased evoked activity, and the alpha/beta oscillations were related to conscious perception, and not the coordination of motor actions.

3.4. Neural correlates of full vs partial consciousness

The final aim of the study was to understand how cortical activity differed between full and partial consciousness. The difference in partial and full conscious perception being a graded phenomenon posed a problem for identifying their neuronal correlates, as only very few responses of the same physical strength were differentially rated either fully or partially perceived. To account for the effect of contrast strengths between the fully and partially perceived stimuli, we next investigated changes in evoked activity and oscillation amplitudes in only high contrast stimuli (179 ± 91 trials for each subject) (Fig. 5). In trials where participants rated the stimuli as fully visible, compared to trials in which the stimuli were rated as partially visible, significant increases in evoked activity was observed between 0.2 and 0.4 s, and between 0.6 and 0.8 s (Fig. 5A). Early increases in the ER was localized to fronto-parietal regions such as the fronto-marginal gyrus (mrgF), inferior parietal gyrus (iPG), and middle-anterior cingulate (aCIm) (Fig. 5B) while during the later time window ER was also observed in higher visual and inferior temporal regions, such as anterior occipital sulcus (aOS) and middle temporal gyrus (mTG), in addition to superior and inferior frontal gyurs (s/iFG).

Oscillation amplitudes for high contrast stimuli between fully visible and partially visible stimuli showed modulations in narrow-band theta activity (6–7 Hz) (Fig. 5C). Similar to the ER, the theta-band increases were observed late between 0.5 and 0.8 s from stimulus onset. This increase was observed in occipital and temporal regions, such as primary visual cortex (V1) and occipito-temporal gyrus (OTG) as well as parietal regions, such as the post-central and pre-central gyrus (Fig. 5D).

For comparative purposes, we also compared high-contrast, fully perceived stimuli with low-contrast, partially perceived stimuli (317 ± 128 trials for each subject). Full consciousness was associated with a significantly stronger evoked response compared to

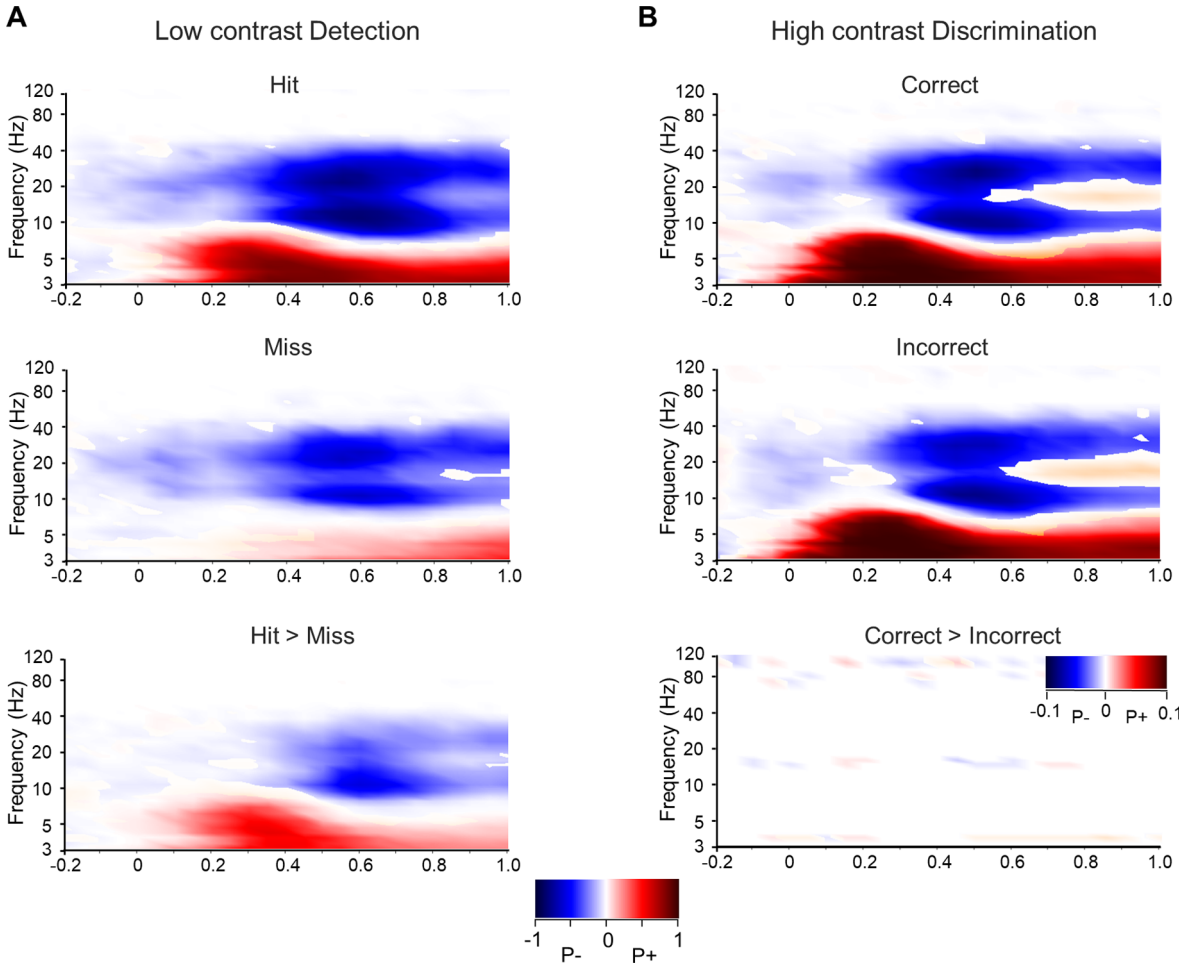

Fig. 3. *Oscillation amplitudes are modulated by partial consciousness and object discrimination.* **(A)** Partial consciousness was estimated as a difference in the responses between Hit and Miss low-contrast stimuli. Time-frequency representation (TFR) of oscillation amplitude modulations for Low contrast Detection Hit trials, Detection Miss trials, and for the difference between Hit and Miss trials. Red colors denote the fraction of cortical parcels where the amplitude was greater (positive tail, P+) and blue colors where the amplitude was smaller (negative tail, P-) compared to the prestimulus baseline or between stimulus conditions (Wilcoxon signed rank test, $p < 0.05$, FDR corrected). Partial compared to null consciousness was associated with sustained increase in theta-band amplitudes and concurrent wide-band amplitude suppression between 8 and 40 Hz **(B)** Same as in A, but for object discrimination. TFRs show amplitude modulations for correct discrimination, incorrect discrimination, and difference between correct and incorrect discrimination for high contrast stimuli. Oscillation amplitudes were not correlated with object discrimination. (For interpretation of the references to color in this figure legend, the reader is referred to the web version of this article.)

partial consciousness, with a peak at around 0.2 s and a smaller peak at 0.4–0.6 s (Fig. 6A). Increased evoked activity for high contrast stimuli was localized to early visual areas and the latter time-window also to lateral occipito-temporal sulcus (laOTS) and lPFC (Fig. 6B). In addition, transient modulations of theta oscillation amplitudes as well as late onset increase in alpha and beta band amplitudes were stronger for full compared to partial consciousness (Fig. 6C). Interestingly, induced beta-band amplitudes that were exclusively found for full conscious perception were localized to the occipitotemporal visual areas including laOTS, medial occipitotemporal sulcus (meOTS) and iTS, as well as to PPC and lPFC (Fig. 6D). We cannot, however, exclude the possibility that these effects were not due to differences in the contrast strengths rather than the difference between full and partial consciousness.

3.5. Oscillation amplitudes in the theta band and evoked activity are correlated with subjective visibility ratings

To reveal if subjective visibility would also be correlated with the strength of neuronal responses, we first estimated the individual distributions of visibility ratings that were provided at the conclusion of each trial (Fig. 7A). For the low contrast condition, participants rated stimuli as not visible (mean = 52.7%, bias-corrected and accelerated [Bca] 95%CI = [41.1–62.4]) and barely visible (mean = 39.5%, Bca 95%CI = [29.1–41.4]) but not partially or fully visible. In contrast and as expected, for the high contrast condition, participants mostly rated stimuli as fully (mean = 31.2%, Bca 95%CI = [21.8–42.5]) and partially visible

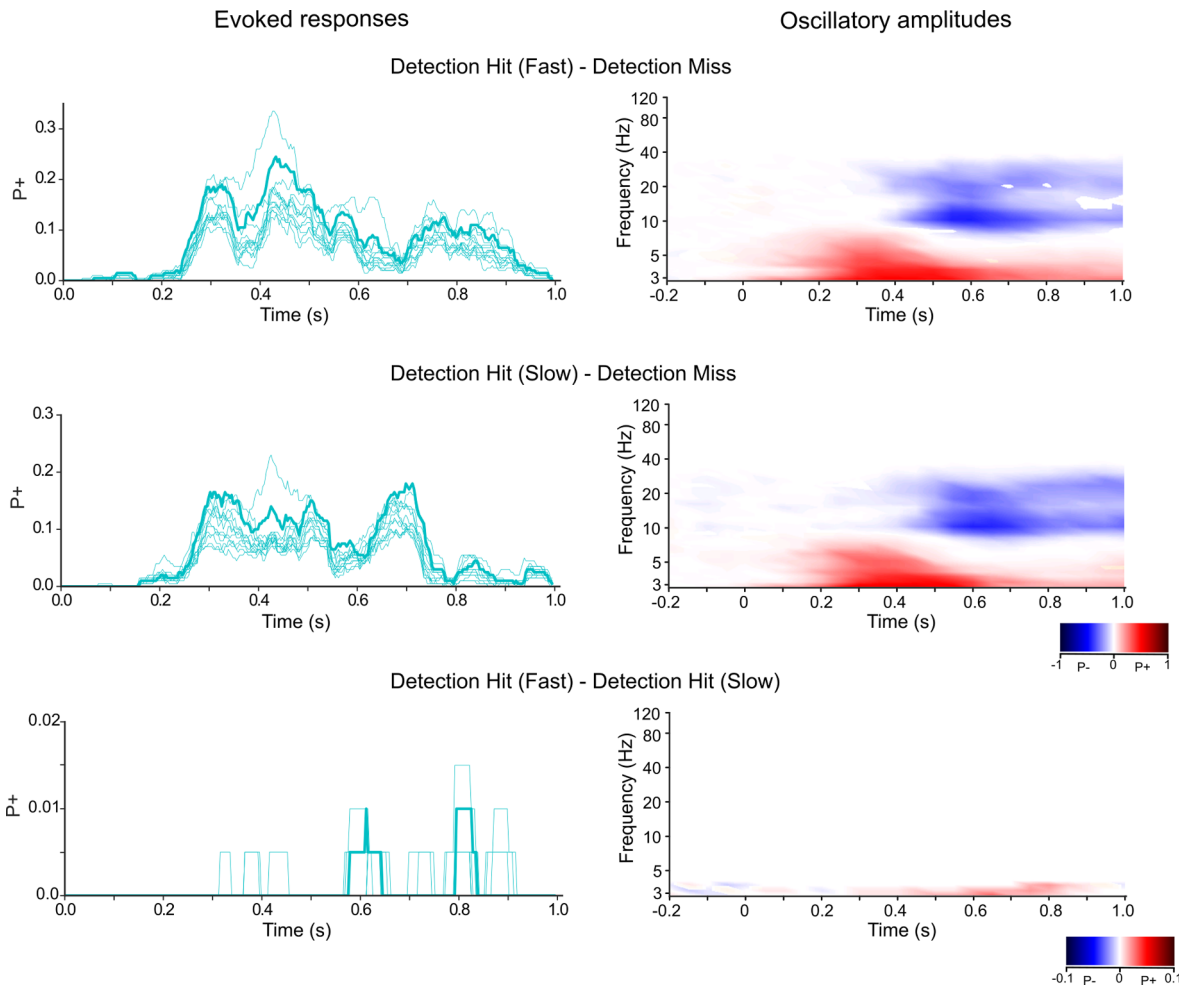

Fig. 4. *Correlation of post-stimulus dynamics with reaction times.* A fraction of the brain areas in which evoked responses and oscillation amplitudes of Detection Hit trials, were significantly different from Detection Miss trials separately for fast and slow RTs, (Evoked responses: *T*-test, $p < .01$, cluster corrected; Oscillation amplitudes: Wilcoxon signed rank test, $p < 0.05$, FDR corrected). The trials were split at the median RT of each subject and the mean of these median RTs was 0.907 ± 0.144 s (mean ± SD across subjects). Bottom row shows the fraction of brain areas in which the evoked responses and oscillation amplitudes were significantly different between fast and slow trials of Detection Hit (Evoked responses: *T*-test, $p < .01$, cluster corrected; Oscillation amplitudes: Wilcoxon signed rank test, $p < 0.05$, FDR corrected).

(mean = 51.1%, Bca 95%CI = [42.7–60.5]) with a minority of trials being rated as barely visible (mean = 16.1%, Bca 95%CI = [8.8–27.8]).

A Pearson randomization test ($p < 0.01$) was subsequently used to test whether subjective visibility, regardless of the contrast strength, was correlated with the strength of ERs (Fig. 7B) and oscillation amplitudes (Fig. 7C) (159 ± 72 trials for each subject). Both ERs and theta-band amplitudes showed sustained correlation with the visibility ratings across the visual system but also in PPC and lPFC (Fig. 7D–E). To further investigate whether the correlation with visibility was due to differences in contrast strength or by the actual visibility, we plotted the mean strengths of the significant regions for all of the subjective visibility ratings. We deduced that if the correlation was due to contrast strengths, the distribution of the strengths should be bimodal and clearly separate low- and high contrast stimuli (as in Fig. 7A) while if it was due to differences in visibility the correlation should be linear and not show a clear distinction between low- and high contrast trials.

Both the ERs and theta band amplitudes increased as a function of visibility (Fig. 7F–G). Regression analysis was used to fit the evoked responses and theta band amplitudes to the curve of best fit. The evoked responses were fit with a quadratic regression model, indicating decreased differences between the ER of partially and fully visible stimuli. The theta-band amplitudes, however, displayed a linear relationship, indicating that oscillation amplitudes were not fully dependent on contrast strengths but rather on the visibility ratings from 'Not visible' to 'Fully visible'. In contrast, the ERs were more reflecting changes in contrast strengths albeit with a small component reflecting also changes in visibility.

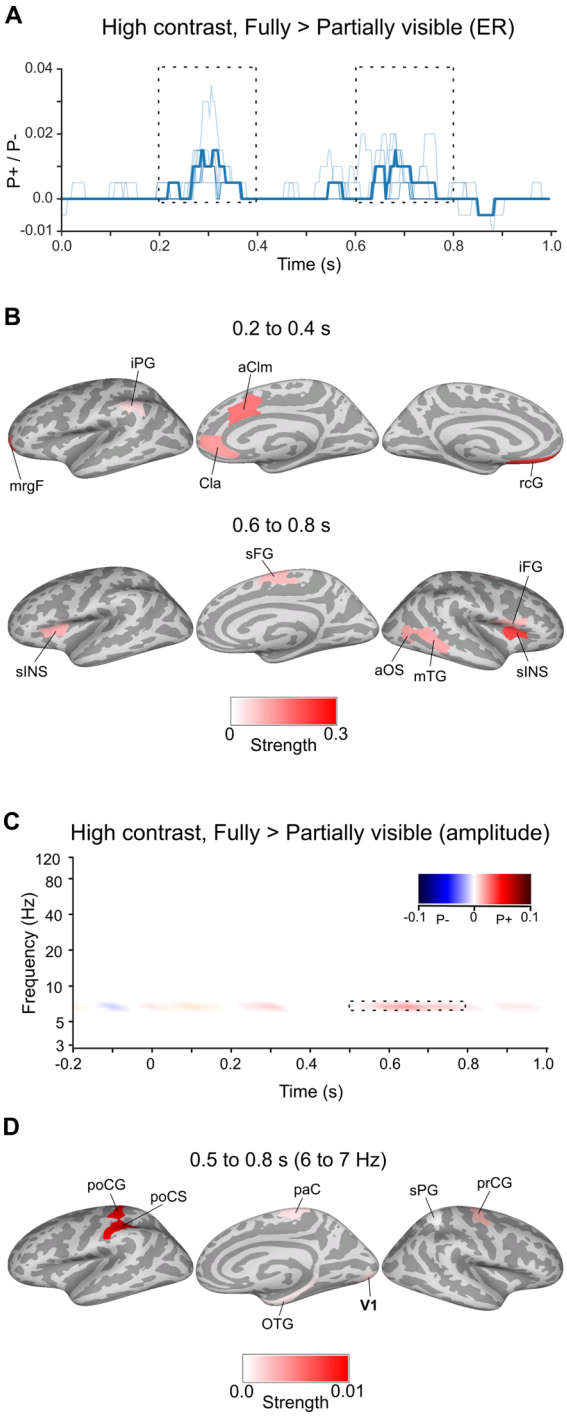

Fig. 5. *ERs and oscillation amplitudes for fully visible compared to partially visible high contrast trials.* **(A)** A fraction of the brain areas (parcels) in which ERs were significantly different when the stimuli was rated as fully visible compared to when the stimuli was rated as partially visible for high contrast trials (*T*-test, $p < .05$, cluster corrected) as a function of time. Positive values (P +) indicate significant increases in evoked activity in fully visible compared to partially visible trials, while negative values (P −) indicate significant decreases in evoked activity. **(B)** The cortical areas in which evoked activity was stronger for Fully visible compared to Partially visible trials over the 0.2–0.4 s and 0.6–0.8 s time windows. Colors of the parcels indicate average strength of the evoked activity over the time window. **(C)** TFRs of amplitude modulations that were significantly different for Fully visible trials compared to Partially visible trials (Wilcoxon signed rank, $p < .05$, FDR corrected). **(D)** The cortical areas in which increased amplitude in 6.5 Hz were observed in the 0.5–0.8 s time window. Parcels are indicated with acronyms: fronto-marginal gyrus (mrgF), anterior cingulate (CIa), middle-anterior cingulate (aCIm), gyrus rectus (rcG), paracentral lobule (paC), and occipito-temporal gyrus (OTG), anterior occipital sulcus (aOS), superior insula (sINS), superior parietal gyrus (sPG). Rest of acronyms as in Figs. 2 and 4.

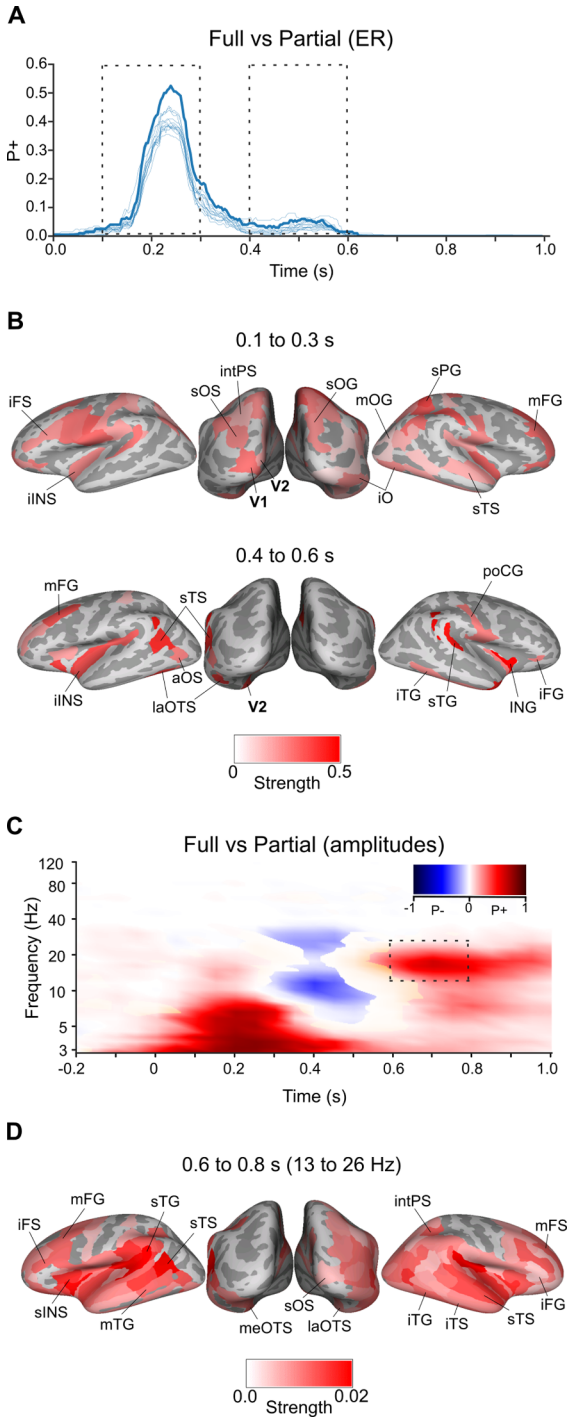

Fig. 6. *ERs and oscillation amplitudes are strengthened in full compared to partial consciousness.* **(A)** A fraction of the brain areas (parcels) in which ERs were stronger for Discrimination Correct trials compared to Detection Hit trials (*T*-test, $p < .01$, cluster corrected) as a function of time. **(B)** The cortical areas in which evoked activity was stronger for Discrimination Correct compared to Detection Hit over the 0.1–0.3 s and 0.4–0.6 s time windows. **(C)** TFRs of amplitude modulations that were significantly different for Discrimination Correct trials compared to Detection Hit trials (Wilcoxon signed rank test, $p < .05$, FDR corrected). **(D)** The cortical areas in which increased beta-band (13–26 Hz) amplitudes were observed in the 0.6–0.8 s time window. Parcels are indicated with acronyms: inferior insula (iINS), lateral occipital temporal sulcus (laOTS), medial occipito-temporal sulcus (meOTS), lateral sulcus (laSp), and inferior temporal sulcus (iTS). Rest of acronyms as in Figs. 2, 4, and 5.

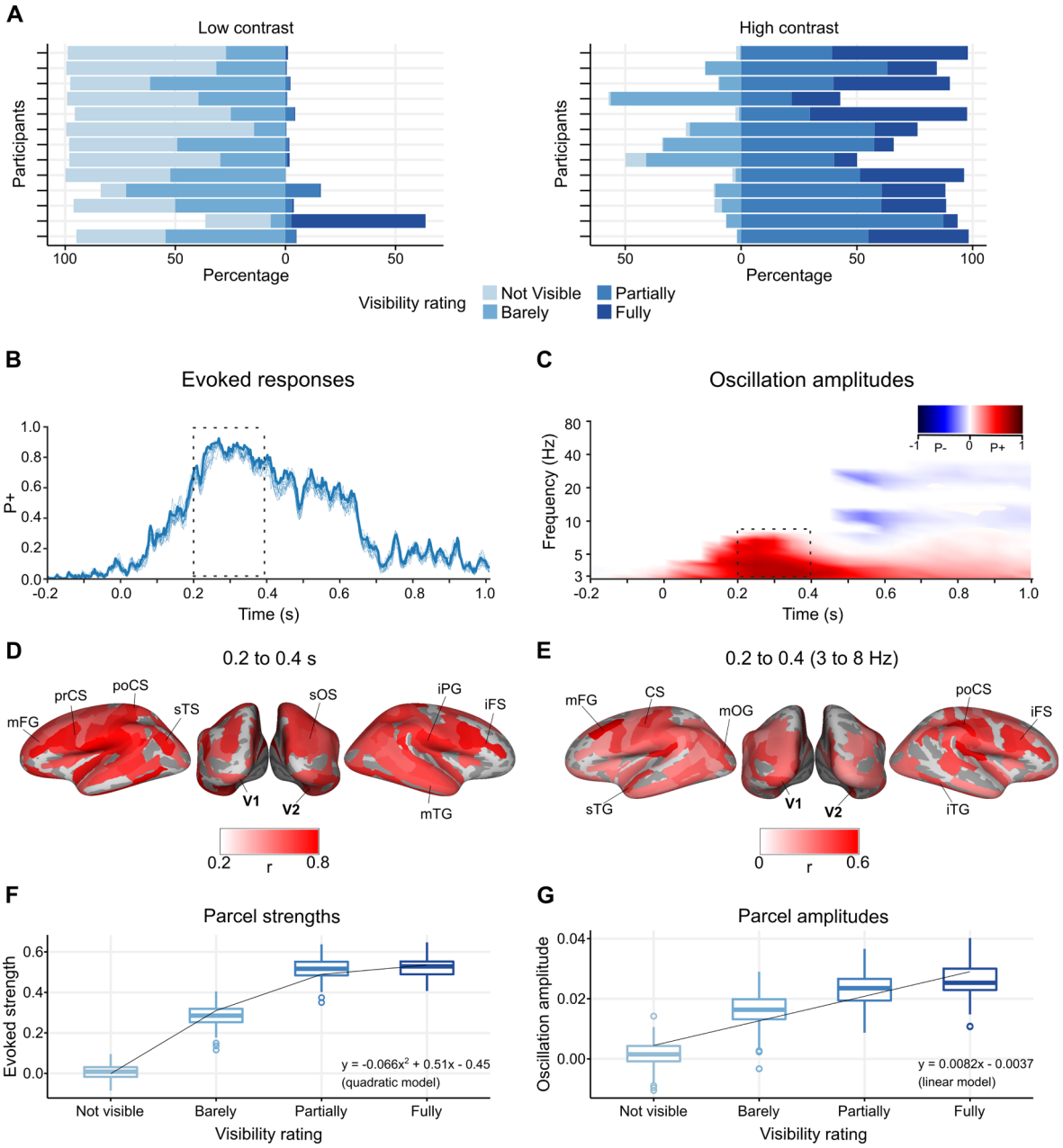

Fig. 7. *ERs and oscillation amplitudes are correlated with participants' visibility ratings.* **(A)** Distribution of visibility ratings for each participant and contrast condition. Participants rated Low contrast stimuli predominantly as Not Visible or Barely Visible. Conversely, they rated High contrast stimuli predominantly as Partially Visible or Fully Visible. **(B)** A fraction of the brain areas (parcels) in which the strength of ER between Not Visible, Barely Visible, Partially Visible, and Fully Visible conditions were significantly correlated (Pearson randomization test, $p < .01$, FDR corrected). Dashed square indicates time period used in D to visualize significant parcels. **(C)** TFR of the correlation between oscillation amplitudes with the participants' visibility ratings (Pearson randomization test, $p < .01$, FDR corrected). The transient early theta amplitudes were correlated with the visibility ratings. Dashed square indicates the time-frequency window used in E to visualize parcels in which significant correlations were observed. **(D)** The cortical parcels in which significant positive correlation between ER and visibility ratings were observed between 0.2 and 0.4 s. **(E)** The cortical parcels in which significant positive correlation between amplitude and visibility ratings were observed between 0.2 and 0.4 s and 3–8 Hz. **(F)** Strength of the evoked response averaged over significant parcels in D for each visibility rating. Regression analysis was used to fit the trajectory of evoked strength to a quadratic curve. **(G)** Same as F, but for theta-band amplitudes. The parcel amplitudes were fit with a linear regression model. Parcels are indicated with acronyms: precentral sulcus (prCS), postcentral sulcus (poCS), central sulcus (CS). Rest of acronyms as in Figs. 2–6.

4. Discussion

We used source-reconstructed MEG data to investigate differences in the evoked activity and oscillation amplitudes between fully and partially perceived visual stimuli. Both partial and full conscious perception were associated with long-lasting evoked activity. Critically, the cortical sources of both partial and full conscious perception were distributed throughout the brain from the visual system to PPC and PFC, supporting the idea that conscious perception arises from "broadcasting" information across brain regions (Dehaene & Changeux, 2011; Sergent & Dehaene, 2004b; van Vugt et al., 2018). The cortical sources of full compared to partial visual perception were, however, localized to the higher-order visual system.

4.1. Visual perception is a graded phenomenon

Our behavioral results indicate that visual perception is a graded process both at the objective and subjective level. The two interleaved Bayesian staircases we used to determine individual thresholds (objective performance of 50% detection and 77% correct discrimination) displayed very distinct performance profiles across all participants. Objective measures of awareness indicated that subjects had greater sensitivity and lower response bias for high than low-contrast stimuli. Furthermore, when stimulus strength was such that only 50% of stimuli were detected, stimulus identification was at chance-level. Participants were thus only partially aware of stimuli at perceptual threshold: they were aware of a perceptual experience, but did not have a precise representation of its content. Such chance level detection performance at perceptual threshold is in line with previous results using simple unmasked stimuli (Koivisto et al., 2017; Tagliabue et al., 2016) and higher order masked stimuli (Magazzini, Ruhnau, & Weisz, 2016). When stimulus strength was calibrated to achieve above-chance level identification, the perceptual experience becomes vivid enough that nearly all stimuli were identified so that participants were fully aware of both the perceptual experience and its contents. Such phenomena where stimuli are only sometimes detected if they are not identified and always detected when they are identified indicates that the difference in partial and full conscious perception is a graded phenomenon (Grill-Spector & Kanwisher, 2005; Sekar et al., 2013; Sergent & Dehaene, 2004a). This dichotomy between partial and full consciousness was also present in subjective measures of awareness. Participants rated seen low contrast stimuli almost exclusively as barely visible while they rated high contrast stimuli mostly as partially or fully visible. In line with previous research (Andersen, Pedersen, Sandberg, & Overgaard, 2015; Overgaard et al., 2006; Sandberg et al., 2011), perception of simple visual stimuli displayed a transition from the barely perceptible experience of partial consciousness to the detailed experience of full consciousness. These results are similar to recent findings using the multiple object tracking paradigm which found that participants can be aware of stimulus location but not of its identity (Wu & Wolfe, 2018).

4.2. Partial consciousness is correlated with early widespread cortical activation

When participants were able to detect but not identify the visual stimuli, increased evoked activity dissociated seen and unseen stimuli. Using spectral analysis of oscillation amplitudes, we further found sustained theta (3–7 Hz) band increase along with wide-band amplitude suppression from 10 to 40 Hz to dissociate visual conscious perception from unseen visual stimuli. Evoked activity differentiating seen and unseen stimuli peaked at 300 and 400 ms from stimulus onset, corresponding to N200 and P3 that are known correlates of visual conscious perception in prior EEG (Del Cul et al., 2007; Koivisto et al., 2008; Rutiku, Aru, & Bachmann, 2016; Eklund & Wiens, 2018) and MEG sensor-level data (Andersen et al., 2015; Sandberg et al., 2013; Sandberg, Barnes, Rees, & Overgaard, 2014; Sekar et al., 2013).

While many studies have found gamma (30–120 Hz) amplitudes to be correlated with conscious perception in MEG sensor-level (Palva, Linkenkaer-Hansen et al., 2005; Wyart & Tallon-Baudry, 2008) and iEEG (Aru et al., 2012; Fisch et al., 2009; Gaillard et al., 2009; Vidal et al., 2014; Vidal et al., 2015) data, we found no evidence for the hypothesis that gamma amplitudes are correlated with conscious perception *per se,* as indicated by partial consciousness. In contrast, we used MEG source reconstruction to identify cortical regions underlying visual conscious perception and found evoked activity as well as sustained theta oscillations to be larger for the consciously perceived than unperceived stimuli. This activity was observed both in primary and in ventral visual stream regions higher in the cortical processing hierarchy, as well as intPS of PPC and in lPFC. These findings are well in agreement with those from iEEG (Gaillard et al., 2009; Noy et al., 2015) and for somatosensory perception (Hirvonen & Palva, 2016) but differ from a prior study that used MEG source-reconstruction and found only occipital sources (Andersen et al., 2015).

Our data supports the model of conscious perception where frontal cortex plays a key role in supporting the emergence of conscious percepts (Dehaene, Sergent, & Changeux, 2003; Dehaene & Changeux, 2011; Del Cul, Dehaene, Reyes, Bravo, & Slachevsky, 2009; Gaillard et al., 2009). The widespread and early increase of evoked activity and oscillation amplitudes supports the neural 'ignition' model where large-scale reverberating activity characterizes the transition from null to partial consciousness and marks the shift between the lack of any conscious percept to a perceptual experience, however faint the awareness may be (Dehaene & Changeux, 2011; van Vugt et al., 2018).

4.3. Neural correlates of full consciousness

We also compared neuronal activity between full and partial consciousness between different contrast strengths as had been done in some previous studies (King, Pescetelli, & Dehaene, 2016; Tagliabue et al., 2016) and found beta-oscillations (13–26 Hz) and evoked activity to be stronger for the high-contrast fully perceived than for the low-contrast partially perceived stimuli. This is in line

with prior studies that have found the amplitude modulations of beta and gamma oscillations to be correlated with conscious sensory perception in sensor-level MEG (Schurger, Cowey, & Tallon-Baudry, 2006; Wyart & Tallon-Baudry, 2008), and iEEG (Aru et al., 2012; Fisch et al., 2009; Gaillard et al., 2009; Lachaux et al., 2005; Vidal et al., 2015; Herman et al., 2019) data. Beta oscillations were found in lateral occipito-temporal areas that underlie object recognition (Bar et al., 2001; Cichy, Chen, & Haynes, 2011; Grill-Spector, Kushnir, Hendler, & Malach, 2000; Orlov & Zohary, 2018), suggesting that they could be related to the representation of stimulus features and stimulus information as found previously (Grutzner et al., 2013; Honkanen et al., 2015; Palva, Linkenkaer-Hansen et al., 2005; Singer, 1999; Tallon-Baudry, Bertrand, Peronnet, & Pernier, 1998). The activation of frontoparietal regions in both evoked activity and in theta and beta oscillations was similar to that observed to characterize full conscious perception in several prior studies involving fMRI (Blankenburg et al., 2003; Dehaene & Changeux, 2011; Hegner, Lindner, & Braun, 2016; Li Hegner, Lindner, & Braun, 2015), iEEG (Fisch et al., 2009; Gaillard et al., 2009) and source-reconstructed MEG data (Hirvonen & Palva, 2016; King et al., 2016; Salti et al., 2015). The preceding studies have shown that local neuronal activity in frontoparietal regions, together with that in sensory areas, is positively correlated with conscious perception. However, it cannot be excluded that the beta oscillations in our study reflect only increases in the contrasts strengths and further studies are needed to resolve this issue.

Correct identification compared to incorrect identification of stimulus identity for high contrast visual stimuli was associated only with an increase in evoked activity between 400 and 600 ms from stimulus onset in middle occipital sulcus (mOS) of the visual system, as well as in post-central gyrus (poCG) and iFS. The weak differences between correctly and incorrectly identified visual stimuli are not surprising taken that this difference is primarily due to differences in visual perception rather than differences in conscious perception *per se*. This view is supported by the localization of the difference between correct and incorrect identification to mOS and iFS, as they have been shown to be sensitive to stimulus features (Kravitz et al., 2013; Munk et al., 2002) and may hence here be related to the processing of stimulus identity in conscious perception. Interestingly, iFS and poCG are also key hubs in the attention networks (Corbetta & Shulman, 2002), which suggests a contribution of attentional top-down modulation to object identification.

4.4. Evoked activity and theta oscillations dissociate full from partial consciousness

The problem for identifying neuronal correlates of partial and full visual conscious perception was that few responses of the same physical strength were differentially rated either full or partially perceived. In full consciousness, participants were able to both consciously perceive and correctly identify a stimuli, while in partial consciousness, participants perceived a stimuli but were not able to report its identity. We hence compared neuronal activity for high contrast stimuli that were either fully or partially perceived. Here both early and late evoked activity and late theta-band oscillations were stronger for the fully than partially perceived stimuli. This is in agreement with prior data that have found enhanced theta oscillations for conscious somatosensory awareness (Hirvonen, Monto, Wang, Palva, & Palva, 2018; Hirvonen & Palva, 2016) and to be correlated with subjective reports of words reported as perceived (Melloni et al., 2007). The late response is in line with prior studies involving stimulus identification that have observed late correlates of full consciousness (Del Cul et al., 2007; Gaillard et al., 2009; Levy, Vidal, Fries, Démonet, & Goldstein, 2015; Wyart & Tallon-Baudry, 2008). Conversely, these results imply that during early visual processing, stimulus is only coarsely experienced and finer representations of the sensory properties of the object occur only at later time points (Koivisto et al., 2017; Mack, Gauthier, Sadr, & Palmeri, 2008). These data together suggest that the key components dissociating full and partial visual conscious perception, independently of visual contrast, are the late evoked activity between 400 and 600 ms after stimulus onset together with enhanced theta-band oscillations.

Cortical regions in which neuronal activity dissociated full from partial conscious perception were V1 and anterior occipital sulcus in the visual system as well as iPG, PoCG/S, iFGm, and sFG that belong to fronto-parietal attention networks frequently associated with conscious perception (Dehaene et al., 2003; Dehaene & Changeux, 2011; Del Cul et al., 2009; Gaillard et al., 2009). Interestingly, the anterior cingulate and insula also showed increased evoked activity to fully compared to partially perceived visual stimuli. Anterior cingulate has been linked to perceptual consciousness in prior fMRI and single neuron recordings indicating the key role of this region in signaling the content of conscious perception (Chica, Bayle, Botta, Bartolomeo, & Paz-Alonso, 2016; Gelbard-Sagiv, Mudrik, Hill, Koch, & Fried, 2018). Moreover, both anterior cingulate and insula have been associated with mind-body associations (Popa et al., 2019) and with self-awareness (Park et al., 2018) suggesting, together with our data, that the activity of these regions is related to the richness of perceptual experiences.

Evoked activity and sustained theta amplitudes were also correlated with participants' visibility reports. As the strength of theta-band amplitudes increased linearly with visibility, this increase in the strength cannot be explained by differences in contrast strengths. However, the increase in ERs reflected changes in contrast strengths but also in visibility, as found in prior sensor-level EEG (Tagliabue et al., 2016) and MEG (Andersen et al., 2015) studies where the strength of ERs were correlated with ratings in the perceptual awareness scale (PAS). Since ERs were correlated with contrast strength and slightly with subjective visibility scores, ERs likely reflect the intensity of stimulus representations rather than the coding of object identity *per se*. Similar to prior fMRI studies that have found BOLD activity in distributed brain regions being correlated with graded visual perception (Binder et al., 2017; Christensen et al., 2006; Imamoglu et al., 2014), our results showed that correlation of visibility with theta oscillations is found in a distributed network across the visual system, PPC, and PFC, and of which activity may reflect the intensity of the conscious experience.

4.5. Evoked activity and theta oscillations as part of NCC

We found that both evoked activity and sustained theta/low-alpha oscillations could be part of the NCC. In addition to the NCC, post-stimulus activity following conscious perception can also be confounded by a response requirement (Tsuchiya et al., 2015) and

the consequences following consciousness (NCC-co) (Aru, Bachmann, Singer, & Melloni, 2012; Pitts, Martinez, & Hillyard, 2012; Tsuchiya et al., 2015). However, the independence of the ERs or oscillation amplitudes on response RTs and the similarity of these post-perceptual processing for the fast and slow response trials suggest that theta/low alpha-band amplitudes and ERs are part of the NCC for conscious visual perception. Further evidence for ERs and theta/low-alpha band oscillations was gained from the comparison between full and partial conscious perception for high contrast stimuli (Fig. 5) as well as between the contrast strengths (Fig. 6) that were associated with identical response requirements and post-perceptual processing but yet revealed very similar patterns of evoked and oscillatory activity as a correlate of conscious perception. These results are in line with prior EEG studies that have shown that early (Koivisto, Salminen-Vaparanta, Grassini, & Revonsuo, 2016; Ye & Lyu, 2019) and late (Eklund, Gerdfeldter, & Wiens, 2019) neural correlates of conscious perception are not related to response requirement.

5. Conclusions

We used MEG to reveal neuronal correlates of partial and full visual conscious perception and their differences. NCC for partial consciousness included increased early evoked activity, sustained increase in theta/low-alpha band amplitudes, and a wideband suppression of oscillation amplitudes. NCC for full conscious perception was additionally associated with a late increase in both beta band amplitudes and late evoked activity. Yet, NCC for full compared to partial conscious perception differed only by the stronger evoked activity and theta oscillations for full conscious perception. These data are in line with the view that the neuronal contents of conscious sensory perception (characterized by full consciousness) are distinct from awareness itself (partial consciousness) (Aru et al., 2012; Pitts, Padwal, Fennelly, Martinez, & Hillyard, 2014; Vidal et al., 2015), as well as with the partial awareness hypothesis which posits that the levels of awareness depend on which representational levels can be accessed (Kouider et al., 2010).

Declaration of Competing Interest

The authors declare that they have no known competing financial interests or personal relationships that could have appeared to influence the work reported in this paper.

Acknowledgements

This study was supported by the Academy of Finland (SA 266402, 1303933 and SA 325404 to SP and SA 253130 and 256472 to MP). The authors declare no competing financial interests.

Appendix A. Supplementary material

Supplementary data to this article can be found online at https://doi.org/10.1016/j.concog.2019.102863.

References

Andersen, L. M., Pedersen, M. N., Sandberg, K., & Overgaard, M. (2015). Occipital MEG activity in the early time range (< 300 ms) predicts graded changes in perceptual consciousness. *Cerebral Cortex, 26*(6), 2677–2688.

Aru, J., Axmacher, N., Do Lam, A. T., Fell, J., Elger, C. E., Singer, W., & Melloni, L. (2012). Local category-specific gamma band responses in the visual cortex do not reflect conscious perception. *The Journal of Neuroscience: The Official Journal of the Society for Neuroscience, 32*(43), 14909–14914. https://doi.org/10.1523/JNEUROSCI.2051-12.2012.

Aru, J., Bachmann, T., Singer, W., & Melloni, L. (2012). Distilling the neural correlates of consciousness. *Neuroscience and Biobehavioral Reviews, 36*(2), 737–746. https://doi.org/10.1016/j.neubiorev.2011.12.003.

Bar, M., Tootell, R. B., Schacter, D. L., Greve, D. N., Fischl, B., Mendola, J. D., ... Dale, A. M. (2001). Cortical mechanisms specific to explicit visual object recognition. *Neuron, 29*(2), 529–535 S0896-6273(01)00224-0 [pii].

Binder, M., Gociewicz, K., Windey, B., Koculak, M., Finc, K., Nikadon, J., ... Cleeremans, A. (2017). The levels of perceptual processing and the neural correlates of increasing subjective visibility. *Consciousness and Cognition, 55*, 106–125.

Blankenburg, F., Taskin, B., Ruben, J., Moosmann, M., Ritter, P., Curio, G., & Villringer, A. (2003). Imperceptible stimuli and sensory processing impediment. *Science (New York, N.Y.), 299*(5614), 1864. https://doi.org/10.1126/science.1080806.

Block, N. (2005). Two neural correlates of consciousness. *Trends in Cognitive Sciences, 9*(2), 46–52.

Brainard, D. H. (1997). The psychophysics toolbox. *Spatial Vision, 10*, 433–436.

Bullmore, E., & Sporns, O. (2009). Complex brain networks: Graph theoretical analysis of structural and functional systems. *Nature Reviews. Neuroscience, 10*(3), 186–198. https://doi.org/10.1038/nrn2575.

Chica, A. B., Bayle, D. J., Botta, F., Bartolomeo, P., & Paz-Alonso, P. M. (2016). Interactions between phasic alerting and consciousness in the fronto-striatal network. *Scientific Reports, 6*, 31868. https://doi.org/10.1038/srep31868.

Christensen, M. S., Ramsøy, T. Z., Lund, T. E., Madsen, K. H., & Rowe, J. B. (2006). An fMRI study of the neural correlates of graded visual perception. *NeuroImage, 31*(4), 1711–1725.

Cichy, R. M., Chen, Y., & Haynes, J. D. (2011). Encoding the identity and location of objects in human LOC. *NeuroImage, 54*(3), 2297–2307. https://doi.org/10.1016/j.neuroimage.2010.09.044.

Corbetta, M., & Shulman, G. L. (2002). Control of goal-directed and stimulus-driven attention in the brain. *Nature Reviews. Neuroscience, 3*(3), 201–215. https://doi.org/10.1038/nrn755.

Dale, A. M., Liu, A. K., Fischl, B. R., Buckner, R. L., Belliveau, J. W., Lewine, J. D., & Halgren, E. (2000). Dynamic statistical parametric mapping: Combining fMRI and MEG for high-resolution imaging of cortical activity. *Neuron, 26*(1), 55–67. https://doi.org/10.1016/S0896-6273(00)81138-1.

Dehaene, S., & Changeux, J. P. (2011). Experimental and theoretical approaches to conscious processing. *Neuron, 70*(2), 200–227. https://doi.org/10.1016/j.neuron.2011.03.018.

Dehaene, S., Sergent, C., & Changeux, J. P. (2003). A neuronal network model linking subjective reports and objective physiological data during conscious perception. *Proceedings of the National Academy of Sciences of the United States of America, 100*(14), 8520–8525. https://doi.org/10.1073/pnas.1332574100 1332574100 [pii].

Del Cul, A., Baillet, S., & Dehaene, S. (2007). Brain dynamics underlying the nonlinear threshold for access to consciousness. *PLoS Biology, 5*(10), e260. https://doi.org/10.1371/journal.pbio.0050260.
Del Cul, A., Dehaene, S., Reyes, P., Bravo, E., & Slachevsky, A. (2009). Causal role of prefrontal cortex in the threshold for access to consciousness. *Brain: A Journal of Neurology, 132*(Pt 9), 2531–2540. https://doi.org/10.1093/brain/awp111.
Destrieux, C., Fischl, B., Dale, A., & Halgren, E. (2010). Automatic parcellation of human cortical gyri and sulci using standard anatomical nomenclature. *NeuroImage, 53*(1), 1–15. https://doi.org/10.1016/j.neuroimage.2010.06.010.
Eklund, R., Gerdfeldter, B., & Wiens, S. (2019). Effects of a manual response requirement on early and late correlates of auditory awareness. *Frontiers in Psychology, 10*, 2083. https://doi.org/10.3389/fpsyg.2019.02083.
Eklund, R., & Wiens, S. (2018). Visual awareness negativity is an early neural correlate of awareness: A preregistered study with two gabor sizes. *Cognitive, Affective & Behavioral Neuroscience, 18*(1), 176–188. https://doi.org/10.3758/s13415-018-0562-z.
Elliott, J. C., Baird, B., & Giesbrecht, B. (2016). Consciousness isn't all-or-none: Evidence for partial awareness during the attentional blink. *Consciousness and Cognition, 40*, 79–85. https://doi.org/10.1016/j.concog.2015.12.003.
Fahrenfort, J. J., Scholte, H. S., & Lamme, V. A. (2007). Masking disrupts reentrant processing in human visual cortex. *Journal of Cognitive Neuroscience, 19*(9), 1488–1497. https://doi.org/10.1162/jocn.2007.19.9.1488.
Fisch, L., Privman, E., Ramot, M., Harel, M., Nir, Y., Kipervasser, S., ... Malach, R. (2009). Neural "ignition": Enhanced activation linked to perceptual awareness in human ventral stream visual cortex. *Neuron, 64*(4), 562–574. https://doi.org/10.1016/j.neuron.2009.11.001.
Fischl, B. (2012). FreeSurfer. *NeuroImage, 62*(2), 774–781.
Gaillard, R., Dehaene, S., Adam, C., Clemenceau, S., Hasboun, D., Baulac, M., ... Naccache, L. (2009). Converging intracranial markers of conscious access. *PLoS Biology, 7*(3), e61. https://doi.org/10.1371/journal.pbio.1000061.
Gelbard-Sagiv, H., Mudrik, L., Hill, M. R., Koch, C., & Fried, I. (2018). Human single neuron activity precedes emergence of conscious perception. *Nature Communications, 9*(1), https://doi.org/10.1038/s41467-018-03749-0.
Gramfort, A., Luessi, M., Larson, E., Engemann, D. A., Strohmeier, D., Brodbeck, C., ... Hämäläinen, M. S. (2014). MNE software for processing MEG and EEG data. *NeuroImage, 86*, 446–460. https://doi.org/10.1016/j.neuroimage.2013.10.027.
Grill-Spector, K., & Kanwisher, N. (2005). Visual recognition: As soon as you know it is there, you know what it is. *Psychological Science, 16*(2), 152–160 PSCI796 [pii].
Grill-Spector, K., Kushnir, T., Hendler, T., & Malach, R. (2000). The dynamics of object-selective activation correlate with recognition performance in humans. *Nature Neuroscience, 3*(8), 837–843. https://doi.org/10.1038/77754.
Grutzner, C., Wibral, M., Sun, L., Rivolta, D., Singer, W., Maurer, K., & Uhlhaas, P. J. (2013). Deficits in high- (> 60 hz) gamma-band oscillations during visual processing in schizophrenia. *Frontiers in Human Neuroscience, 7*, 88. https://doi.org/10.3389/fnhum.2013.00088.
Hegner, Y. L., Lindner, A., & Braun, C. (2016). A somatosensory-to-motor cascade of cortical areas engaged in perceptual decision making during tactile pattern discrimination. *Human Brain Mapping*. https://doi.org/10.1002/hbm.23446.
Hirvonen, J., Monto, S., Wang, S., Palva, J., & Palva, S. (2018). Dynamic large-scale network synchronization from perception to action. *Network Neuroscience, 2*(4), 442–463. https://doi.org/10.1162/netn_a_00039.
Hirvonen, J., & Palva, S. (2016). Cortical localization of phase and amplitude dynamics predicting access to somatosensory awareness. *Human Brain Mapping, 37*(1), 311–326. https://doi.org/10.1002/hbm.23033.
Honkanen, R., Rouhinen, S., Wang, S. H., Palva, J. M., & Palva, S. (2015). Gamma oscillations underlie the maintenance of feature-specific information and the contents of visual working memory. *Cerebral Cortex (New York, N.Y.: 1991), 25*(10), 3788–3801. https://doi.org/10.1093/cercor/bhu263.
Imamoglu, F., Heinzle, J., Imfeld, A., & Haynes, J. (2014). Activity in high-level brain regions reflects visibility of low-level stimuli. *NeuroImage, 102*, 688–694.
Jones, S. R., Pritchett, D. L., Stufflebeam, S. M., Hamalainen, M., & Moore, C. I. (2007). Neural correlates of tactile detection: A combined magnetoencephalography and biophysically based computational modeling study. *The Journal of Neuroscience : The Official Journal of the Society for Neuroscience, 27*(40), 10751–10764. https://doi.org/10.1523/JNEUROSCI.0482-07.2007.
King, J. R., Pescetelli, N., & Dehaene, S. (2016). Brain mechanisms underlying the brief maintenance of seen and unseen sensory information. *Neuron, 92*(5), 1122–1134 S0896-6273(16)30801-7 [pii].
Koivisto, M., Grassini, S., Salminen-Vaparanta, N., & Revonsuo, A. (2017). Different electrophysiological correlates of visual awareness for detection and identification. *Journal of Cognitive Neuroscience, 29*(9), 1621–1631.
Koivisto, M., Salminen-Vaparanta, N., Grassini, S., & Revonsuo, A. (2016). Subjective visual awareness emerges prior to P3. *European Journal of Neuroscience, 43*(12), 1601–1611.
Koivisto, M., Lahteenmaki, M., Sorensen, T. A., Vangkilde, S., Overgaard, M., & Revonsuo, A. (2008). The earliest electrophysiological correlate of visual awareness? *Brain and Cognition, 66*(1), 91–103 S0278-2626(07)00097-8 [pii].
Korhonen, O., Palva, S., & Palva, J. M. (2014). Sparse weightings for collapsing inverse solutions to cortical parcellations optimize M/EEG source reconstruction accuracy. *Journal of Neuroscience Methods, 226C*, 147–160. https://doi.org/10.1016/j.jneumeth.2014.01.031.
Kouider, S., De Gardelle, V., Sackur, J., & Dupoux, E. (2010). How rich is consciousness? The partial awareness hypothesis. *Trends in Cognitive Sciences, 14*(7), 301–307.
Kravitz, D. J., Saleem, K. S., Baker, C. I., Ungerleider, L. G., & Mishkin, M. (2013). The ventral visual pathway: An expanded neural framework for the processing of object quality. *Trends in Cognitive Sciences, 17*(1), 26–49. https://doi.org/10.1016/j.tics.2012.10.011.
Kulashekhar, S., Pekkola, J., Palva, J. M., & Palva, S. (2016). The role of cortical beta oscillations in time estimation. *Human Brain Mapping, 37*(9), 3262–3281. https://doi.org/10.1002/hbm.23239.
Lachaux, J. P., George, N., Tallon-Baudry, C., Martinerie, J., Hugueville, L., Minotti, L., ... Renault, B. (2005). The many faces of the gamma band response to complex visual stimuli. *NeuroImage, 25*(2), 491–501. https://doi.org/10.1016/j.neuroimage.2004.11.052.
Levy, J., Vidal, J. R., Fries, P., Démonet, J., & Goldstein, A. (2015). Selective neural synchrony suppression as a forward gatekeeper to piecemeal conscious perception. *Cerebral Cortex, 26*(7), 3010–3022.
Li Hegner, Y., Lindner, A., & Braun, C. (2015). Cortical correlates of perceptual decision making during tactile spatial pattern discrimination. *Human Brain Mapping, 36*(9), 3339–3350. https://doi.org/10.1002/hbm.22844.
Lobier, M., Palva, J. M., & Palva, S. (2017). High-alpha band synchronization across frontal, parietal and visual cortex mediates behavioral and neuronal effects of visuospatial attention. *NeuroImage, 165*, 222–237 S1053-8119(17)30871-6 [pii].
Mack, M. L., Gauthier, I., Sadr, J., & Palmeri, T. J. (2008). Object detection and basic-level categorization: Sometimes you know it is there before you know what it is. *Psychonomic Bulletin & Review, 15*(1), 28–35. https://doi.org/10.3758/pbr.15.1.28.
Magazzini, L., Ruhnau, P., & Weisz, N. (2016). Alpha suppression and connectivity modulations in left temporal and parietal cortices index partial awareness of words. *NeuroImage, 133*, 279–287. https://doi.org/10.1016/j.neuroimage.2016.03.025.
Maris, E., & Oostenveld, R. (2007). Nonparametric statistical testing of EEG-and MEG-data. *Journal of Neuroscience Methods, 164*(1), 177–190.
Melloni, L., Molina, C., Pena, M., Torres, D., Singer, W., & Rodriguez, E. (2007). Synchronization of neural activity across cortical areas correlates with conscious perception. *The Journal of Neuroscience: The Official Journal of the Society for Neuroscience, 27*(11), 2858–2865. https://doi.org/10.1523/JNEUROSCI.4623-06.2007.
Melloni, L., Schwiedrzik, C. M., Muller, N., Rodriguez, E., & Singer, W. (2011). Expectations change the signatures and timing of electrophysiological correlates of perceptual awareness. *The Journal of Neuroscience: The Official Journal of the Society for Neuroscience, 31*(4), 1386–1396. https://doi.org/10.1523/JNEUROSCI.4570-10.2011.
Moradi, F., Liu, L. C., Cheng, K., Waggoner, R. A., Tanaka, K., & Ioannides, A. A. (2003). Consistent and precise localization of brain activity in human primary visual

cortex by MEG and fMRI. *NeuroImage, 18*(3), 595–609 S1053811902000538 [pii].
Munk, M. H., Linden, D. E., Muckli, L., Lanfermann, H., Zanella, F. E., Singer, W., & Goebel, R. (2002). Distributed cortical systems in visual short-term memory revealed by event-related functional magnetic resonance imaging. *Cerebral Cortex (New York, N.Y.: 1991), 12*(8), 866–876.
Nieuwenhuis, S., & de Kleijn, R. (2011). Consciousness of targets during the attentional blink: A gradual or all-or-none dimension? *Attention, Perception & Psychophysics, 73*(2), 364–373. https://doi.org/10.3758/s13414-010-0026-1.
Noy, N., Bickel, S., Zion-Golumbic, E., Harel, M., Golan, T., Davidesco, I., ... Malach, R. (2015). Ignition's glow: Ultra-fast spread of global cortical activity accompanying local "ignitions" in visual cortex during conscious visual perception. *Consciousness and Cognition, 35*, 206–224. https://doi.org/10.1016/j.concog.2015.03.006.
Oostenveld, R., Fries, P., Maris, E., & Schoffelen, J. M. (2011). FieldTrip: Open source software for advanced analysis of MEG, EEG, and invasive electrophysiological data. *Computational Intelligence and Neuroscience, 2011*, 156869. https://doi.org/10.1155/2011/156869.
Orlov, T., & Zohary, E. (2018). Object representations in human visual cortex formed through temporal integration of dynamic partial shape views. *The Journal of Neuroscience: The Official Journal of the Society for Neuroscience, 38*(3), 659–678. https://doi.org/10.1523/JNEUROSCI.1318-17.2017.
Overgaard, M., Rote, J., Mouridsen, K., & Ramsøy, T. Z. (2006). Is conscious perception gradual or dichotomous? A comparison of report methodologies during a visual task. *Consciousness and Cognition, 15*(4), 700–708.
Palva, S., Palva, S., Linkenkaer-Hansen, K., Näätänen, R., & Palva, J. M. (2005). Early neural correlates of conscious somatosensory perception. *Journal of Neuroscience, 25*(21), 5248–5258.
Palva, S., Kulashekhar, S., Hamalainen, M., & Palva, J. M. (2011). Localization of cortical phase and amplitude dynamics during visual working memory encoding and retention. *The Journal of Neuroscience: The Official Journal of the Society for Neuroscience, 31*(13), 5013–5025. https://doi.org/10.1523/JNEUROSCI.5592-10.2011.
Palva, S., Linkenkaer-Hansen, K., Naatanen, R., & Palva, J. M. (2005). Early neural correlates of conscious somatosensory perception. *The Journal of Neuroscience: The Official Journal of the Society for Neuroscience, 25*(21), 5248–5258. https://doi.org/10.1523/JNEUROSCI.0141-05.2005.
Park, H. D., Bernasconi, F., Salomon, R., Tallon-Baudry, C., Spinelli, L., Seeck, M., ... Blanke, O. (2018). Neural sources and underlying mechanisms of neural responses to heartbeats, and their role in bodily self-consciousness: An intracranial EEG study. *Cerebral Cortex (New York, N.Y.: 1991), 28*(7), 2351–2364. https://doi.org/10.1093/cercor/bhx136.
Pitts, M. A., Martinez, A., & Hillyard, S. A. (2012). Visual processing of contour patterns under conditions of inattentional blindness. *Journal of Cognitive Neuroscience, 24*(2), 287–303. https://doi.org/10.1162/jocn_a_00111.
Pitts, M. A., Padwal, J., Fennelly, D., Martinez, A., & Hillyard, S. A. (2014). Gamma band activity and the P3 reflect post-perceptual processes, not visual awareness. *NeuroImage, 101*, 337–350. https://doi.org/10.1016/j.neuroimage.2014.07.024.
Popa, I., Barborica, A., Scholly, J., Donos, C., Bartolomei, F., Lagarde, S., ... Mindruta, I. (2019). Illusory own body perceptions mapped in the cingulate cortex-an intracranial stimulation study. *Human Brain Mapping, 40*(9), 2813–2826. https://doi.org/10.1002/hbm.24563.
Ramsøy, T. Z., & Overgaard, M. (2004). Introspection and subliminal perception. *Phenomenology and the Cognitive Sciences, 3*(1), 1–23.
Rodgers, J. L. (1999). The bootstrap, the jackknife, and the randomization test: A sampling taxonomy. *Multivariate Behavioral Research, 34*(4), 441–456. https://doi.org/10.1207/S15327906MBR3404_2.
Rouder, J. N., Speckman, P. L., Sun, D., Morey, R. D., & Iverson, G. (2009). Bayesian t tests for accepting and rejecting the null hypothesis. *Psychonomic Bulletin & Review, 16*(2), 225–237.
Rouhinen, S., Panula, J., Palva, J. M., & Palva, S. (2013). Load dependence of beta and gamma oscillations predicts individual capacity of visual attention. *The Journal of Neuroscience: The Official Journal of the Society for Neuroscience, 33*(48), 19023–19033. https://doi.org/10.1523/jneurosci.1666-13.2013.
Rutiku, R., Aru, J., & Bachmann, T. (2016). General markers of conscious visual perception and their timing. *Frontiers in Human Neuroscience, 10*, 23.
Salti, M., Monto, S., Charles, L., King, J. R., Parkkonen, L., & Dehaene, S. (2015). Distinct cortical codes and temporal dynamics for conscious and unconscious percepts. *eLife, 4*. https://doi.org/10.7554/eLife.05652.
Sandberg, K., Bahrami, B., Kanai, R., Barnes, G. R., Overgaard, M., & Rees, G. (2013). Early visual responses predict conscious face perception within and between subjects during binocular rivalry. *Journal of Cognitive Neuroscience, 25*(6), 969–985. https://doi.org/10.1162/jocn_a_00353.
Sandberg, K., Barnes, G. R., Rees, G., & Overgaard, M. (2014). Magnetoencephalographic activity related to conscious perception is stable within individuals across years but not between individuals. *Journal of Cognitive Neuroscience, 26*(4), 840–853. https://doi.org/10.1162/jocn_a_00525.
Sandberg, K., Bibby, B. M., Timmermans, B., Cleeremans, A., & Overgaard, M. (2011). Measuring consciousness: Task accuracy and awareness as sigmoid functions of stimulus duration. *Consciousness and Cognition, 20*(4), 1659–1675. https://doi.org/10.1016/j.concog.2011.09.002.
Sandberg, K., Timmermans, B., Overgaard, M., & Cleeremans, A. (2010). Measuring consciousness: Is one measure better than the other? *Consciousness and Cognition, 19*(4), 1069–1078. https://doi.org/10.1016/j.concog.2009.12.013.
Schurger, A., Cowey, A., & Tallon-Baudry, C. (2006). Induced gamma-band oscillations correlate with awareness in hemianopic patient GY. *Neuropsychologia, 44*(10), 1796–1803 S0028-3932(06)00085-6 [pii].
Sekar, K., Findley, W. M., Poeppel, D., & Llinas, R. R. (2013). Cortical response tracking the conscious experience of threshold duration visual stimuli indicates visual perception is all or none. *Proceedings of the National Academy of Sciences of the United States of America, 110*(14), 5642–5647. https://doi.org/10.1073/pnas.1302229110.
Sergent, C., Baillet, S., & Dehaene, S. (2005). Timing of the brain events underlying access to consciousness during the attentional blink. *Nature Neuroscience, 8*(10), 1391–1400 nn1549 [pii].
Sergent, C., & Dehaene, S. (2004a). Is consciousness a gradual phenomenon? Evidence for an all-or-none bifurcation during the attentional blink. *Psychological Science JID – 9007542, 15*(11), 720–728.
Sergent, C., & Dehaene, S. (2004b). Neural processes underlying conscious perception: Experimental findings and a global neuronal workspace framework. *Journal of Physiology, 98*(4–6), 374–384. https://doi.org/10.1016/j.jphysparis.2005.09.006 S0928-4257(05)00025-2 [pii].
Siebenhühner, F., Wang, S. H., Palva, J. M., & Palva, S. (2016). Cross-frequency synchronization connects networks of fast and slow oscillations during visual working memory maintenance. *eLife, 5*, e13451. https://doi.org/10.7554/eLife.13451.
Singer, W. (1999). Neuronal synchrony: A versatile code for the definition of relations? *Neuron, 24*(1), https://doi.org/10.1016/s0896-6273(00)80821-1 pp. 49–65, 111–25.
Sokal, R. R., & Rohlf, F. J. (1995). *Biometry: The principles and practice of statistics in biological research* (3rd ed.). New York, USA: W. H. Freeman.
Stanislaw, H., & Todorov, N. (1999). Calculation of signal detection theory measures. *Behavior Research Methods, Instruments, & Computers: A Journal of the Psychonomic Society Inc, 31*(1), 137–149.
Tagliabue, C. F., Mazzi, C., Bagattini, C., & Savazzi, S. (2016). Early local activity in temporal areas reflects graded content of visual perception. *Frontiers in Psychology, 7*, 572.
Tallon-Baudry, C., Bertrand, O., Peronnet, F., & Pernier, J. (1998). Induced gamma-band activity during the delay of a visual short-term memory task in humans. *The Journal of Neuroscience: The Official Journal of the Society for Neuroscience, 18*(11), 4244–4254.
Taulu, S., Simola, J., & Kajola, M. (2005). Applications of the signal space separation method. *IEEE Transactions on Signal Processing, 53*(9), 3359–3413.
Tsuchiya, N., Wilke, M., Frässle, S., & Lamme, V. A. (2015). No-report paradigms: Extracting the true neural correlates of consciousness. *Trends in Cognitive Sciences, 19*(12), 757–770.
van Vugt, B., Dagnino, B., Vartak, D., Safaai, H., Panzeri, S., Dehaene, S., & Roelfsema, P. R. (2018). The threshold for conscious report: Signal loss and response bias in visual and frontal cortex. *Science (New York, N.Y.), 360*(6388), 537–542. https://doi.org/10.1126/science.aar7186.
Vidal, J. R., Perrone-Bertolotti, M., Kahane, P., & Lachaux, J. P. (2015). Intracranial spectral amplitude dynamics of perceptual suppression in fronto-insular, occipito-

temporal, and primary visual cortex. *Frontiers in Psychology, 5*, 1545. https://doi.org/10.3389/fpsyg.2014.01545.
Vidal, J. R., Perrone-Bertolotti, M., Levy, J., De Palma, L., Minotti, L., Kahane, P., ... Lachaux, J. P. (2014). Neural repetition suppression in ventral occipito-temporal cortex occurs during conscious and unconscious processing of frequent stimuli. *NeuroImage, 95*, 129–135. https://doi.org/10.1016/j.neuroimage.2014.03.049.
Wu, C. C., & Wolfe, J. M. (2018). A new multiple object awareness paradigm shows that imperfect knowledge of object location is still knowledge. *Current Biology: CB, 28*(21) 3430–3434.e3 S0960-9822(18)31126-6 [pii].
Wyart, V., & Tallon-Baudry, C. (2008). Neural dissociation between visual awareness and spatial attention. *The Journal of Neuroscience: The Official Journal of the Society for Neuroscience, 28*(10), 2667–2679. https://doi.org/10.1523/JNEUROSCI.4748-07.2008.
Herman, X. W., Smith, R. E., Kronemer, S. I., Watsky, R. E., Chen, W. C., Gober, M. L., ... Blumenfeld, H. (2017). A switch and wave of neuronal activity in the cerebral cortex during the first second of conscious perception. *Cerebral Cortex (New York, N.Y.: 1991),* 1–14. https://doi.org/10.1093/cercor/bhx327.
Ye, M., & Lyu, Y. (2019). Later positivity reflects post-perceptual processes: Evidence from immediate detection and delayed detection tasks. *Frontiers in Psychology, 10*, 82. https://doi.org/10.3389/fpsyg.2019.00082.
Yeo, B. T., Krienen, F. M., Sepulcre, J., Sabuncu, M. R., Lashkari, D., Hollinshead, M., ... Buckner, R. L. (2011). The organization of the human cerebral cortex estimated by intrinsic functional connectivity. *Journal of Neurophysiology, 106*(3), 1125–1165. https://doi.org/10.1152/jn.00338.2011.